BMC Genomics

RESEARCH

Open Access

# Single-cell transcriptomic and chromatin accessibility atlas of peripheral blood mononuclear cells reveals immune cell heterogeneity and breed-specific characteristics in Duroc and Meishan pigs

Hairui Fan[1,2†], Cui Du[2†], Chao Xu[1†], Haifei Wang[1], Yejun Wang[3], Zhengchang Wu[1], Bin Zhao[4], Chao Chen[5], Shaobin Shang[2], Ming-an Sun[2*] and Wenbin Bao[1*]

## Abstract

**Background** Pig is an important model for biomedical studies, yet the immune cell heterogeneity, the subtle relationship between immune cells and the inter-breed immune variation in pigs remains poorly characterized. Here, we generate single-cell transcriptomes for the Peripheral Blood Mononuclear Cells (PBMCs) of two pig breeds with distinct immune traits including Duroc and Meishan pigs – with the latter have better immune capacity.

**Results** Dozens of cell types are annotated, with γδ T lymphocytes making up one-fifth of all PBMCs. A list of putative novel markers is identified in each cell type, such as *GATA3*, *SYTL3* and *C9H1orf186* which are enriched in γδ T lymphocytes. The cellular composition and immune gene expression abundance are compared across breeds, showing that Meishan pigs have higher proportion of monocytes and their monocytes have enhanced expression of immune-related genes. Re-clustering analysis further identified the sub-populations of T, B and monocytes, with their inter-breed differences further characterized. We also generate single-cell chromatin maps for PBMCs of Duroc pigs and identify a list of transcription factors associated with each immune lineage. Comparison with human data demonstrates that while most cell populations and the corresponding markers match between pig and human, $CD4^+CD8^+$ DPTCs and γδ T cells are absent in human and one monocyte subset are absent in pigs.

**Conclusions** Overall, the present study examined the transcription levels and constructed the single-cell maps of blood immune cells between Duroc and Meishan pigs, which revealed the heterogeneity of immune cells in pigs

†Hairui Fan, Cui Du and Chao Xu contributed equally to this work.

*Correspondence:
Ming-an Sun
mingansun@yzu.edu.cn
Wenbin Bao
wbbao@yzu.edu.cn

Full list of author information is available at the end of the article

and their differential characteristics among Duroc and Meishan pigs. This observation would be valuable for better understanding of the immune heterogeneity and immune traits in pigs.

**Keywords** PBMC, Immune heterogeneity, ScRNA-seq, ScATAC-seq, Inter-breed immune variation

## Introduction

The domestic pig (*Sus scrofa domesticus*) is one of the most valuable economic animals for meat production [1]. Owing to its similarity to humans in terms of anatomy, genetics, and physiology, it also serves as an advantageous animal model for immunology research and biomedical studies and a favorable resource for organ xenotransplantation [2–4]. Importantly, pigs also have an immune system that closely resembles that of humans, as demonstrated by previous observations that the immune systems of human and pig share many properties that are absent in mouse [5, 6] and larger number of immune genes are conserved between human and pig relative to mouse [7]. Therefore, in-depth investigation of the porcine immune system is not only important for understanding porcine immunity but could also facilitate biomedical studies for human immunity and diseases [2, 8].

Despite of the extraordinary similarity to human, the immune system of pigs also owns some unique properties that are not fully clarified. One striking example is related to γδ T cells, which are a peculiar lineage of T lymphocytes that are important for innate and adaptive immunity [9, 10] and nutrient sensing [11]. This is in contrast to the alternative αβ T lineage that contributes mainly to adaptive immunity. Interestingly, γδ T cells are prominent in pigs to make up 15%–35% of lymphocytes in peripheral blood, yet only represent about 1% of Peripheral Blood Mononuclear Cells (PBMCs) in humans [12–14]. Another example is related to interleukin 4 (IL-4) which stimulates B cells and is essential for antibody product in humans, but plays a opposite role in pigs to suppress antigen-stimulated B cell proliferation and block antibody production [15]. Taken together, pig owns a human-like immune system that also has some unique features the deserve further studies, yet the immune system in pig is still far from as well-characterized as in humans and mice.

During the domestication and breeding of domestic pigs, dozens of breeds have been created that are highly diversified for various phenotypes, including those related to growth rate, reproductive capacity and meat quality [16]. Notably, the immune traits are highly variable among breeds [17–21]. For example, several studies have indicated that the Meishan breed from China has better resistance relative to other breeds such as Duroc and Large White against pathogens including bacteria [22], viruses [18, 23] and protozoa [24]. Several studies have further suggested that the immune traits of pigs are associated with the proportions of neutrophils and monocytes [17] and T cell subsets [25]. One study also identified many of SNPs adjacent to T cell related genes that may influence specific immune traits [25]. Despite of these studies, the molecular mechanisms underlying the extraordinary inter-breed variations of immune traits in pigs remain largely unresolved.

Recent advances in single-cell RNA sequencing (scRNA-seq) enables comprehensive characterization of the heterogeneity of the immune system [26, 27]. Further integration of single-cell Assay for Transposase Accessible Chromatin-sequencing (scATAC-seq) can identify the regulatory elements and upstream regulators for distinct cell subsets [28, 29]. Previous applications of scRNA-seq on human PBMCs demonstrate its power in uncovering novel immune cell subsets [30] and identifying key factors in response to infection by pathogens such as COVID-19 [31, 32] and down syndrome-related lung diseases [33]. Nevertheless, single-cell resolution studies on porcine immune systems are still rare, with only one recent study applying scRNA-seq to PBMCs from crossbred pigs [34], which precluded the possibility to reveal the immune trait variations across breeds. Therefore, it is expected that integration of scRNA-seq and scATAC-seq to different pure porcine breeds could provide finer-resolution annotation of the immune cell populations at both transcriptomic and regulatory levels, and reveal the molecular mechanisms underlying the inter-breed variations of immune traits.

In this study, we applied scRNA-seq to profile the PBMCs from Meishan and Duroc pigs, which are two strains with distinctive immune traits, and applied scATAC-seq to Duroc PBMCs. We expect this study will improve the understanding about the immune heterogeneity and inter-breed immune variations in pigs, and identify novel immune cell sub-populations, signaling pathways and regulators that would facilitate future biomedical studies.

## Materials and methods

### Porcine PBMC isolation

The PBMCs samples from two Duroc pigs and two Meishan pigs, respectively, and isolated from venous blood of healthy pigs using a Ficoll-Hypaque density solution according to standard density gradient centrifugation methods (LSM Lymphocyte Separation Medium, mpbio, Solon, USA). For each sample, cell viability was assessed by Trypan Blue Exclusion Test (cell viability > 95%). To minimize batch effect, all blood samples were collected at

the same time with the following procedures for PBMC isolation, scRNA-Seq and scATAC-Seq library preparation and high-throughput sequencing performed in parallel for all collected samples. The Meishan and Duroc pigs used in this study were obtained from the Kunshan Conservation Farm in Jiangsu Province, China. Blood samples were collected with the assistance of the farm staff.

### scRNA-seq library preparation

The single-cell suspensions not cryopreserved of scRNA-seq samples were converted to barcoded scRNA-seq libraries using the Chromium Single Cell Library Kit v3, Gel Bead and Multiplex Kit, and Chip B Kit (10x Genomics). The poly-adenylated transcripts were reverse-transcribed later. Libraries were prepared by the Chromium Single Cell 5′ Reagent kit according to the manufacturer's protocol (10x Genomics, CA, USA). And then all libraries were sequenced on an Illmina Novaseq 6000 with a read length of 150 bp paired-end reads.

### scATAC-seq library preparation

Part of the prepared PBMCs from two Duroc pigs is separated for ATAC sequencing. All protocols to generate scATAC-seq data on the 10x Chromium platform, including sample preparation, library preparation and instrument and sequencing settings, are described below and are also available here: https://support.10xgenomics.com/single-cell-atac.

#### *Nuclei isolation*

The prepared PBMCs (1,000,000 cells) were added to a 1.5 mL microcentrifuge tube and centrifuged (2000 rpm for 5 min at 4 °C). The supernatant was discarded, and then add 100 µl chilled Lysis Buffer (10 mM Tris-HCl (pH 7.4), 10 Mm NaCl, 3 mM MgCl2, 0.1% Tween-20, 0.1% Nonidet P40 Substitute, 0.01% digitonin and 1% BSA) and pipette-mixed 10 times gently. The optimal lysis time of PBMCs was determined by different incubation times on ice, and found that incubation on ice 5 min could got better lysis. Following lysis, 500 µl Wash Buffer (10 mM Tris-HCl (pH 7.4), 10 mM NaCl, 3 mM MgCl2, 0.1% Tween-20 and 1% BSA) was added and pipette-mixed 10 times gently. Then Nuclei were centrifuged (500 g for 5 min at 4 °C) and the supernatant removed without disrupting the nuclei pellet. Nuclei were resuspended in chilled Diluted Nuclei Buffer (10x Genomics; 2000153) at approximately 5,000–7,000 nuclei per µl based on the starting number of cells, and then immediately used to generate scATAC-seq libraries.

#### *Library construction*

scATAC-seq libraries were prepared according to the Chromium Single Cell ATAC Library Kit (10x Genomics; PN-1000083). Briefly, approximate 20,000 resuspended nuclei per sample were combined with ATAC Buffer (10x Genomics; 2000122) and Tn5 transposase (10x Genomics; 2000123/2000138) to form a transposition mix, which was then incubated for 60 min at 37 °C. A master mix composed of Barcoding Reagent (10x Genomics; 2000124), Reducing Agent B (10x Genomics; 2000087) and Barcoding Enzyme (10x Genomics; 2000125/2000139) was then added to the same tube as transposed nuclei. The resulting solution was loaded onto a Chromium Chip E (10x Genomics; 2000121) in a Chip Holder (10x Genomics; 330019). Vortexed Chromium Single Cell ATAC Gel Beads (10x Genomics; 2000132) and Partitioning Oil (10x Genomics; 220088) were also loaded onto the same Chromium Chip E and placing into a Chromium Single Cell Controller instrument (10x Genomics). Resulting single-cell GEMs were collected at the completion of the run (~7 min) and linear amplification was performed in a C1000 Touch Thermal cycler with 96-Deep Well Reaction Module (Bio-Rad; 1851197). Emulsions were coalesced using the Recovery Agent (10x Genomics; 220016), then subjected to Dynabeads (10x Genomics; PN-2000048) and SPRIselect reagent (Beckman Coulter; B23318) bead clean-ups. Indexed sequencing libraries were constructed by combining the barcoded linear amplification product with a Sample Index PCR Mix comprising SI-PCR Primer B (10x Genomics; 2000128), Amp Mix (10x Genomics; 2000047/2000103). Amplification was performed in a C1000 Touch Thermal cycler with 96-Deep Well Reaction Module. The sequencing libraries were subjected to a final bead clean-up SPRIselect reagent and quantified by quantitative PCR (ABI StepOnePlus Real-Time PCR System, Life Technologies), and then libraries were sequenced on Illumina Novaseq 6000 as 50 bp paired-end reads.

### scRNA-seq data analysis

#### *Pre-processing of raw data*

Cell Ranger v3.1.0 was used to align reads to domestic pig reference genome (release Sscrofa11.1). Cell Ranger then uses the transcript annotation GTF to bucket the reads into exonic, intronic, and intergenic, and by whether the reads align (confidently) to the genome. A read is exonic if at least 50% of it intersects an exon, intronic if it is non-exonic and intersects an intron, and intergenic otherwise.

#### *Doublet detection and data filtering*

We first identified doublets using Scrublet v0.2.3 [35] with settings: expected_doublet_rate = 0.08. After discarding the predicted doublets, the data were further filtered using Seurat v4.3.0 [36] to remove low-quality cells and genes by requiring: (1) nCount_RNA between 1000 and 20,000; (2) nFeature_RNA between 500 and 4000; (3) log10GenesPerUMI > = 0.8; (4) mitoRatio < = 0.1; (5)

genes express in no less than 0.1% of cells. The filtered data were used for further analyses.

#### *Dimensionality reduction and clustering*

We used Seurat v4.3.0 [36] to cluster single cells into distinct cell subsets following previous study [37] with modifications. Cells from all samples were integrated for analysis. We selected the top 2,000 variable genes for dimensionality reduction by PCA. The first 25 PCs were selected according to JackStraw and Elbow plots. Nonlinear dimensional reduction and visualization were performed by UMAP method, with resolution set as 0.5 for initial clustering analyses. Cell clusters were annotated based on known marker genes.

To better characterize the cell subtypes for T cells, B cells and monocytes, we performed re-clustering analyses for each major cell type with UMAP method as aforementioned. According to JackStraw and Elbow plots, the first 22, 21 and 18 PCs were selected for T cell, B cell and monocyte, respectively. Resolution was set as 1 for re-clustering analyses.

#### *Cell marker identification and differential expression analysis*

Marker genes for each cluster are annotated with the *FindAllMarkers* function from Seurat v4.3.0 [36] with default settings. Each cluster was annotated based on known markers for porcine immune cells as collected from previous publications. Differential gene expression analysis between different cell clusters or between different porcine breeds are performed with the *FindMarkers* function from Seurat v4.0.1 [36]. For subpopulations within subclusters that could not yet be precisely named, we labeled and distinguished them using numerical sequences (such as gdT1, gdT2, etc.).

#### *Cell cluster proportion comparison*

We used the *propeller* function from the R package Speckle v1.8.0 [38] to compare the cell cluster proportions between the PBMC scRNA-seq data from Duroc and Meishan pigs, with settings: trend = TRUE, robust = TRUE, transform = "logit".

#### *Cross-species scRNA-Seq integration*

We utilized v4.3.0 [36] for cross-species scRNA-Seq data integration. First, human and pig scRNA-Seq data are processed to only keep genes annotated as 1-to-1 orthologues accordingly to ENSEMBL orthologue annotation. Then, the *FindIntegrationAnchors* function is used to determine the cross-species anchors, and the *IntegrateData* function is used to integrate involved datasets. Finally, the integrated data are scaled followed by dimensionality reduction, clustering and visualization following the same procedure as same-species data integration. The first 25 PCs were selected for use according to JackStraw and Elbow plots. Resolution was set as 0.5 for clustering analyses. Cell cluster annotation was performed based on known markers for human and pig.

### scATAC-seq data analysis

The scATAC-seq data analysis was conducted based on workflows established in our previous research [39], with modifications as detailed below.

#### *Preprocessing and quality control*

Raw scATAC-seq reads were aligned to the domestic pig genome (Sus scrofa, release Sscrofa11.1) using Cell Ranger ATAC (v1.2.0). Downstream processing and analysis were performed using Seurat v4.3.0 and Signac v1.12.0 [40]. Strict quality control was applied to filter out low-quality cells based on the following criteria: (1) number of fragments in peak regions between 3,000 and 30,000; (2) percentage of reads in peaks > 15%; (3) nucleosome signal < 4; and (4) transcription start site (TSS) enrichment score > 3.

#### *Clustering and dimensionality reduction*

Following filtration, the remaining cells were subjected to Latent Semantic Indexing (LSI) [41]. Clustering and dimensionality reduction were performed on the computed LSI components (excluding the first component if highly correlated with sequencing depth). Using a resolution of 0.5 and dimensions 2:30, we identified 20 distinct cell clusters.

#### *Gene activity and peak calling*

Gene activity was quantified by assessing local chromatin accessibility within the gene body and a 2 kb region upstream of the TSS. Accessible chromatin peaks for each cell type were called using MACS2 v2.2.6 [42]. Differential chromatin accessibility analysis was conducted using the FindAllMarkers function with a Bonferroni-adjusted p-value < 0.05 and a $\log_2$ fold change > 0.25 as significance thresholds. Genomic regions harboring accessible chromatin peaks were annotated using ChIPSeeker v1.36.0 [43].

#### *Motif enrichment analysis*

Transcription factor binding motifs were retrieved from the JASPAR 2020 database. Specifically, the 'CORE' collection for vertebrates was selected using the getMatrixSet function from the TFBSTools package. The position frequency matrices (PFMs) were converted to position weight matrices (PWMs), and motif scanning was performed using motifmatchr within the Signac workflow. Motif enrichment analysis was subsequently conducted using the FindMotifs function, which utilizes a hypergeometric test, with GC-content matched background peaks as controls.

### Integration of scRNA-seq and scATAC-seq data

We integrated scRNA-seq and scATAC-Seq data using Seurat v4.3.0 [36]. In brief, we first calculated the activity of each gene based on scATAC-seq data by considering regions with +/- 2 kb of the gene body using the *GeneActivity* function. Then, we applied the *FindTransferAnchors* function to identify the shared feature correlation structure between scRNA-Seq and scATAC-seq data. Finally, we used the TransferData function to assign cell type annotation to each cell profiled with scATAC-seq using scRNA-seq-based annotation as reference. Differential accessibility peaks among the inferred cell clusters are predicted with the *FindAllMarkers* function with cutoff of p_val_adj < 0.001 and avg_log2FC > 0.25.

### Gene Ontology analysis and motif analysis

Gene Ontology enrichment analyses are performed with DAVID bioinformatics resources [44]. Motif enrichment analysis of scATAC-seq peaks is performed with *FindMotifs* function from Signac v1.1.1 [36] with human motifs from JASPAR2020 database [45] as reference.

### Statistical analysis

All statistics analyses were performed with R Statistical Programming Language.

## Results

### Single-cell transcriptomic analysis of PBMCs for Meishan and Duroc pigs

To resolve the immune cell heterogeneity in pigs at single-cell resolution, we performed scRNA-seq and scATAC-seq with the Chromium platform (10x Genomics) for PBMCs from Duroc pigs. We also performed matched scRNA-seq assay for Meishan pigs which possess relatively high immune capacity – aiming at elucidating how distinct immune cell populations are associated with the inter-breed immune trait variations (Fig. 1A). To minimize the batch effects, all the samples were collected, processed and sequenced in parallel. In total, we obtained 2.1 billion pairs of reads for 63,710 single-cell transcriptomes and 21,855 single-cell chromatin accessibility maps (Table S1). These data enable single-cell resolution annotation of the porcine immune cell populations from both transcriptomic and regulatory levels with consideration of the inter-breed immune trait variations.

To obtain a global picture of the immune cell populations in porcine PBMCs, we first pooled the scRNA-seq data from both breeds for unsupervised clustering. Uniform Manifold Approximation and Projection (UMAP) visualization revealed 20 cell clusters which are recurrently represented in all samples and usually with comparable proportions (Fig. 1B; Table S2), suggesting the global similarity of the immune cellular composition across different breeds. We next annotated each cell cluster based on known porcine immune cell markers [46–49]. All the major immune cell populations are identified, including nine T clusters expressing *CD3E*, *CD247* and *TRBC*, four B clusters expressing *CD79B* and *CD19*, one plasma cluster expressing *JCHAIN*, one Natural Killer (NK) cluster expressing *GNLY* and *KLRK1*, two myeloid clusters expressing *CD14* and *LYZ*, two Dendritic Cell (DC) clusters expressing *FLT3* and *IL3RA*, and one platelet-like cluster expressing *PPBP* (Fig. 1C-E). Notably, we also uncover distinctive subsets of T lymphocytes, including γδ T which is of particularly high proportion (16.3% – 46.7%) in pig [13, 14] and $CD4^+$ $CD8^+$ Double-Positive T Cells (DPTCs) known as effector memory T lymphocytes [50, 51]. Distinct subsets of myeloids and B lymphocytes classified by specific markers are also identified.

To uncover putative novel markers for each immune cell type, we identified the genes enriched in each annotated cell cluster. The numbers of enriched genes are highly variable among different cell clusters, with 1,722 genes for cluster $CD8^+$ T 3 yet only 4 for cluster B 3 (Fig. S1; Table S3). Gene ontology (GO) enrichment analyses indicate that in general, the enriched GO terms well reflect the function of each cell cluster. For example, genes enriched in monocyte clusters are associated with functions like myeloid leukocyte activation, inflammatory response and response to virus, and those for αβ T are associated with lymphocyte activation and adaptive immune system (Table S4). Importantly, we also obtained a list of putative novel markers in addition to known ones, such as *GATA3*, *SYTL3* and *C9H1orf186*, which are enriched in the majority of γδ T lymphocytes with high specificity, which may facilitate the experimental investigation of distinct immune cell subpopulations (Fig. S2; Table S3).

### Cellular composition and transcriptional profile of PBMCs underlie the inter-breed immune variations

The immune traits can vary remarkably among different porcine breeds, with Meishan pigs showing better immune capacity relative to other breeds such as Duroc and Large White [18, 22, 23]. To determine how immune cell populations are related to inter-breed immune trait variations, we compared the proportions of each annotated cell cluster between Duroc and Meishan pigs (Fig. 2A). Despite the consistent cellular populations, we observed remarkable divergence in the proportion of specific cell types across breeds. Particularly, the two monocyte clusters are both overrepresented in Meishan pigs relative to Duroc (FDR = 0.0211 for Monocyte 1, FDR = 0.0588 for Monocyte 2). This is in consistency with previous observation that Meishan pigs have higher monocyte counts in blood [17]. In contrast, NK cells are overrepresented in Duroc pigs with marginal significance (FDR

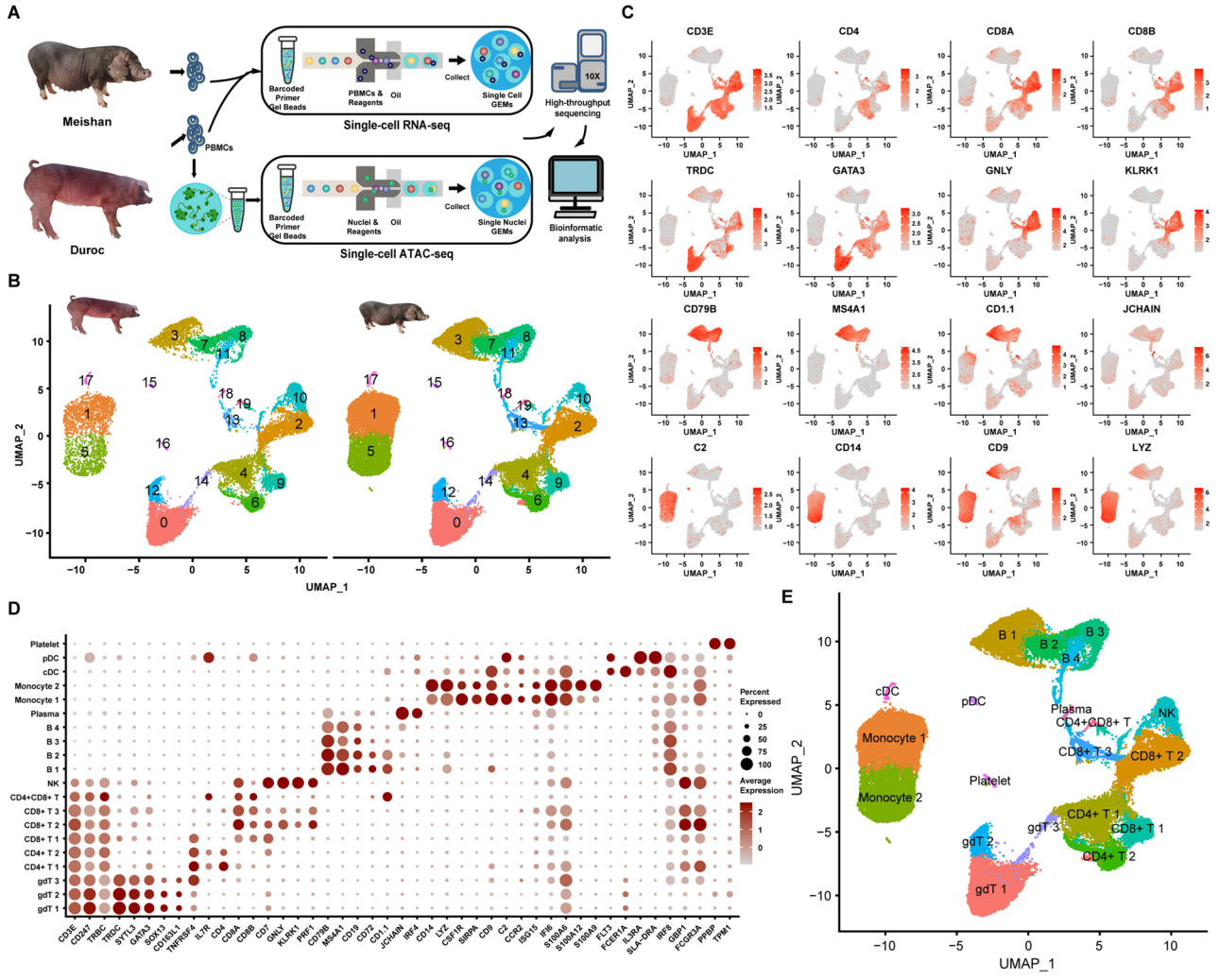


**Fig. 1** Single-cell transcriptional and chromatin accessibility analysis of porcine PBMCs. **A** Scheme showing the preparation of scRNA-Seq and scATAC-Seq data for Duroc and Meishan PBMCs. **B** UMAP visualization based on scRNA-Seq data for porcine PBMCs. Profiled PBMCs for Duroc and Meishan pigs were pooled for clustering, and then visualized separately. **C** UMAP plots for the expression pattern of 20 representative genes across annotated cell clusters. **D** Dot plot for the expression pattern of representative genes across cell clusters. **E** UMAP visualization of profiled PBMCs, with the annotation of each cluster indicated

= 0.0588). Despite the remarkable inter-breed difference for monocytes and NK cells, the adaptive immune cell clusters (i.e., αβ T and B) are presented with similar proportions in these two breeds (Fig. 2A). These results indicate that the inter-breed variations of immune cell composition are largely restricted to innate immune cells.

Intrigued by previous reports that even the same type of immune cells could have remarkable inter-breed immune variations [17, 20], we further identified the differentially expressed genes (DEGs) between Duroc and Meishan pigs for each cell cluster (Fig. 2B-E; Table S5). The numbers of identified DEGs range from 64 to 655 for different clusters (Table S5). GO enrichment analyses suggest that genes overexpressed in the monocytes of Meishan pigs are highly associated with immune-related functions such as granulocyte chemotaxis, response to interferon-gamma and mononuclear cell migration (Fig. 2C). In contrast, genes overexpressed in the monocytes of Duroc pigs are less significantly associated with immune-related functions, and with the adverse function "negative regulation of immune system process" presented (Fig. 2D). Analysis on γδ T cells similarly suggests that genes related to immune activation are overexpressed in Meishan pigs (Fig. S3). In addition, the functions of differentially expressed genes in other cell subpopulations also indicate immune trait variations across pig breeds between the two breeds (Fig. S4,5).

Further inspection confirmed that lots of genes show increased expression in monocytes, T and B lymphocytes, with many of them known to be important for immune response, such as *TMSB15A*, *ISG12(A)*, *FCER1A*, *CD59*, *S100A11* and *LY6E* (Fig. 2B, E-G).

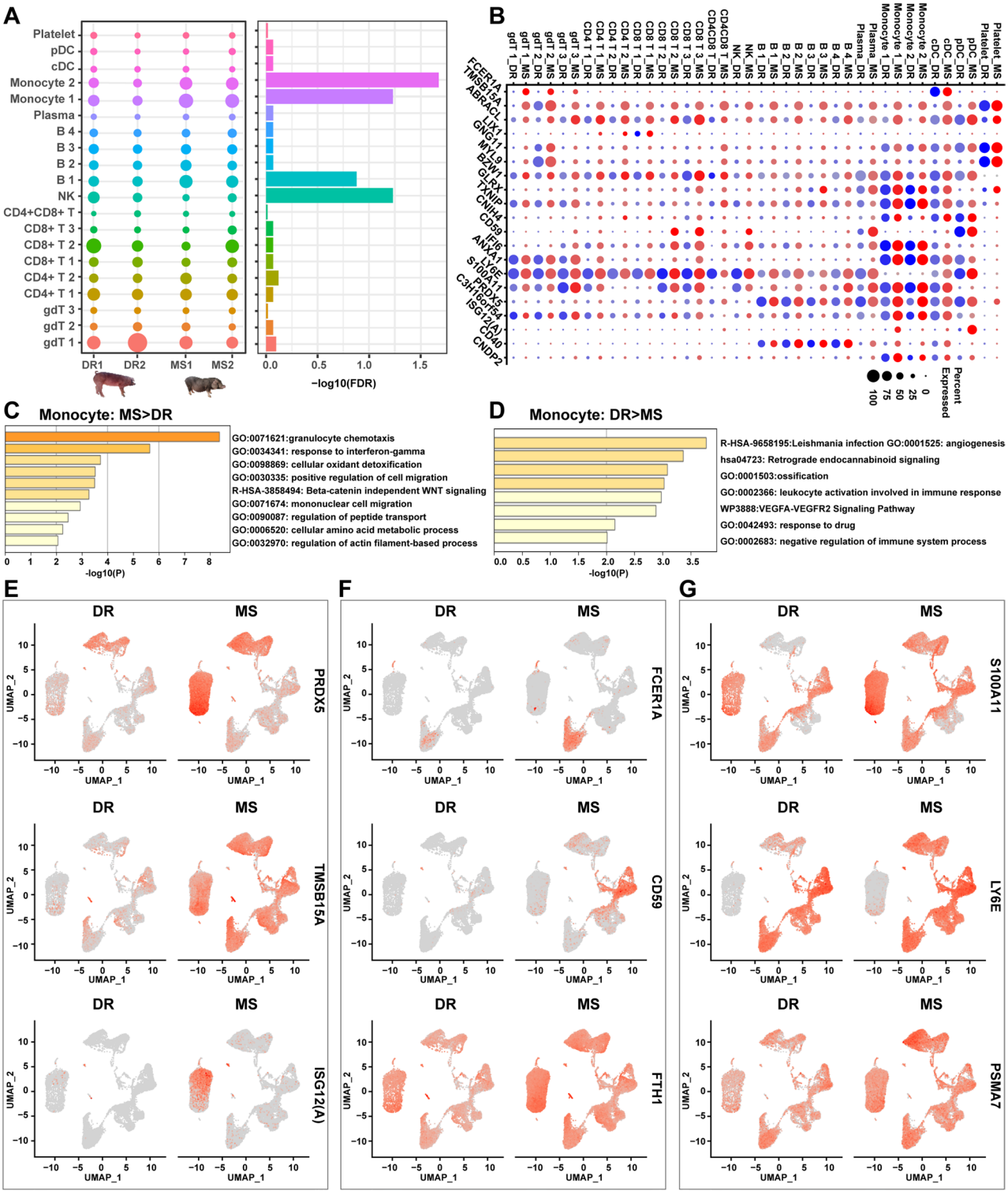


**Fig. 2** Inter-breed variations of cellular compositions and gene expression patterns of PBMCs exist between Duroc and Meishan pigs. **A** Differences of the immune cell composition between Duroc and Meishan pigs. Left panel shows the proportion of each cluster in different samples, right panel indicates the -log10(FDR) and log2fold (MS/DR) as calculated by using *propeller*. **B** Dot plot for the expression differences of representative genes in each cell cluster between Duroc and Meishan pigs. The expression values in Duroc pigs are indicated by blue color, and in Meishan pigs by red color. **C-D** GO enrichment results for the genes overexpressed in the monocytes of Meishan (**C**) and Duroc (**D**) pigs, respectively. **E-G** UMAP plots for the expression distributions of 6 representative genes with higher expression in Meishan relative to Duroc pigs. PRDX5 and TMSB15A have enriched expression in the monocytes of Meishan pigs (**E**), FCER1A and CD59 for the γδ T and $CD8^+$ T/NK of Meishan pigs (**F**), and S100A11 and LY6E for B lymphocytes of Meishan pigs (**G**). DR, Duroc pigs; MS, Meishan pigs

Together, these results indicate that not only the immune cell compositions but also gene expression patterns of counterpart immune cell types may underlie the immune trait variations across pig breeds.

### Heterogeneity and inter-breed differences of myeloid sub-populations

Myeloid cells, which are crucial for innate immunity, make up 21.8% of the profiled porcine PBMCs. Our initial clustering revealed two monocyte subsets, distinguished by CD14 expression (Fig. 1C and D). The $CD14^{hi}$ subset matches classical monocytes (also known as inflammatory monocytes), while the $CD14^{lo}$ subset represents less mature monocytes [52, 53]. Given that the proportions of monocytes show remarkable difference between Duroc and Meishan PBMCs, we performed re-clustering to uncover their sub-clusters and then inspected how the monocyte sub-clusters differ across pig breeds.

Our re-clustering analysis revealed sixteen sub-clusters for monocytes, which were denoted as M1 - M16, respectively (Fig. 3A). The numbers of genes enriched in each cluster range from 22 to 251 (Table S6). Among these clusters, M16 is annotated as neutrophils based on the expression of *HP*, *LCN2*, *PGLYRP1* and *MMP9* [54], and M13 and M14 as myeloid cells mixed with T or B cells respectively based on the expression of corresponding markers (i.e., CD14 for monocyte, CD3E for T and CD79B for B lymphocyte). We focus on the remaining thirteen sub-clusters which are annotated as myeloid cells.

We confirmed the two major monocyte subsets distinguished by the abundance of CD14, denoted as $CD14^{hi}$ (M0, M5, M8, M9, M11) and $CD14^{lo}$ (M1, M2, M3, M4, M6, M7, M12, M15), respectively (Fig. 3B). Unlike in humans which show distinctive *CD16* expression in these two monocyte subsets [52], the expression of CD16 is

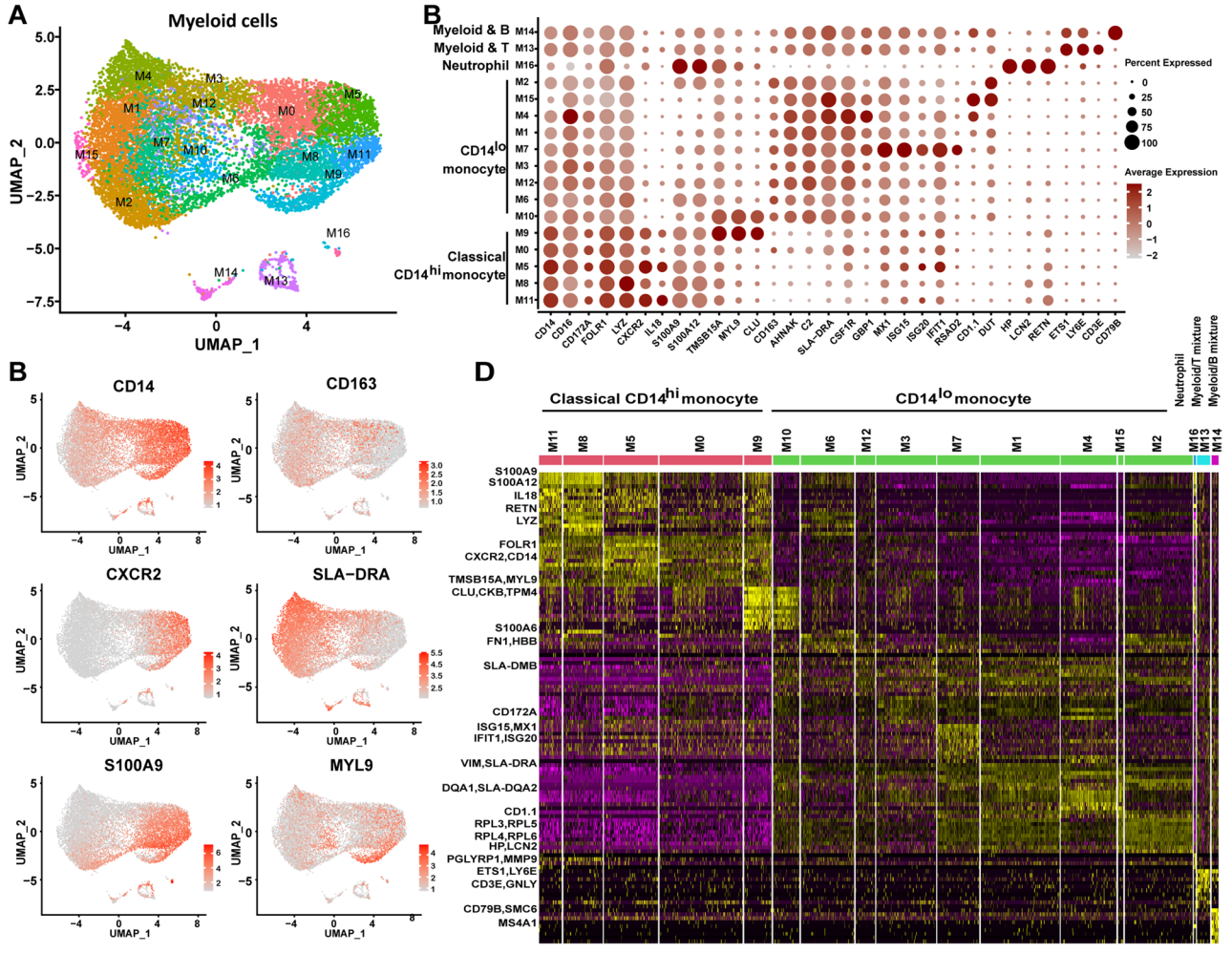


**Fig. 3** Heterogeneity of myeloid in porcine PBMCs revealed by re-clustering analyses. **A** UMAP visualization of myeloid subsets based on re-clustering analysis. **B** UMAP plots for the expression distribution of 6 representative genes among myeloid subsets. **C** Dot plot for the expression pattern of representative genes among different myeloid subsets. **D** Heatmap for the expression pattern of the top 10 genes with enriched expression in each annotated myeloid subset. Color indicates the normalized expression value

comparable in the CD14$^{hi}$ and CD14$^{lo}$ monocytes in pigs (Fig. 3B). We identified many other genes with distinctive expression patterns between these two subsets. For CD14$^{hi}$ subset, we observed enriched expression of *CXCR2*, *IL18* and multiple S100A family members including *S100A6*, *S100A9* and *S100A12* (Fig. 3B-D). However, *CXCR2* is primarily expressed in neutrophils in human [55] which is different from pigs. Furthermore, S100A family members are known as pro-inflammatory factors [56, 57]. For CD14$^{lo}$ monocytes, we observed enriched expression of *CD163*, *C2*, *AHNAK*, *SLA-DRA* and *CSF1R* (Fig. 3B-D). Apart from these two major clusters, we also revealed other distinct sub-clusters, including those marked with *MYL9* and *CLU* (cluster M9 and M10), *MX1*, *ISG15* and *ISG20* (cluster M7), or *DUT* (cluster M2 and M15) (Fig. 3B and D). Together, we uncover distinct subsets of monocytes and demonstrate the prevalence of species-specific markers of myeloid subsets between human and pig.

We then performed inter-breed comparison to reveal the differences for monocyte sub-clusters between Duroc and Meishan pigs. Clustering analysis uncovers the two major groups of monocytes (i.e., CD14$^{hi}$ and CD14$^{lo}$), and demonstrates that all the sub-clusters are shared by Duroc and Meishan pigs (Fig. 4A). We further compared the proportion of each monocyte sub-cluster across breeds. Overall, the monocyte sub-clusters have highly similar proportions for Duroc and Meishan pigs, with only two sub-clusters (M8 and M12, belong to CD14$^{hi}$ and CD14$^{lo}$ groups, respectively) show significantly higher proportions in Meishan pigs (Fig. 4B). These data suggest that the cellular abundance difference mainly occurs for the entire monocyte populations instead of specific monocyte sub-cluster. We further examined the expression pattern for the genes showing enriched expression in each monocyte sub-cluster, and found that all monocyte sub-cluster have highly similar expression profiles in Meishan and Duroc pigs (Fig. 4C). Meanwhile, we also identified 285 genes showing altered expression between Meishan and Duroc pigs, with the numbers of DEGs usually of a few dozen for each sub-cluster (Fig. 4D; Table S7). While most of these genes (e.g., ABRACL and P2RX5) show similar trends in different monocyte sub-clusters regarding their inter-breed expression alterations, we also noticed a few genes (e.g., RETN and S100A9) showing breed-specific expression in only distinct sub-clusters (Fig. 4E, F, S4).

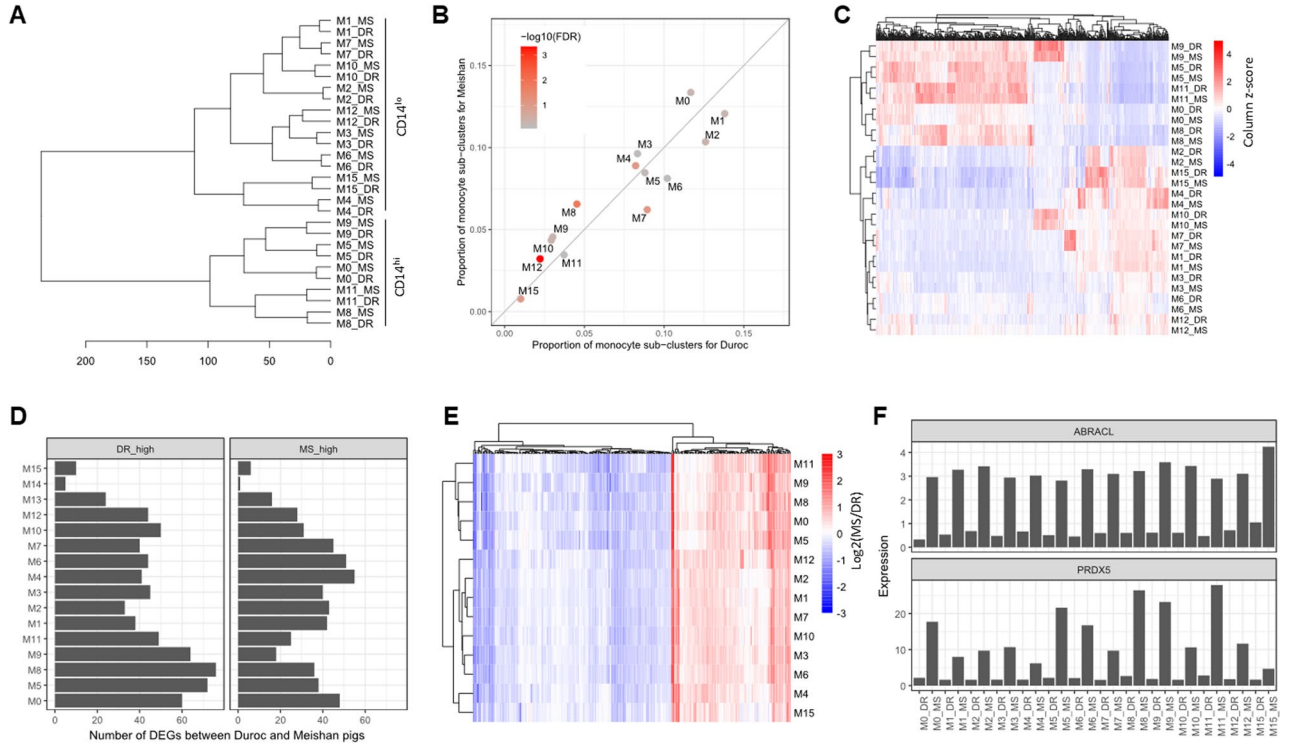


**Fig. 4** Inter-breed differences of cellular proportion and gene expression for myeloid sub-clusters. **A** Hierarchical clustering of monocyte sub-clusters based on their gene expression profiles. **B** Comparison of the cellular proportions of monocyte sub-clusters between Duroc and Meishan pigs. **C** Expression profiles for the marker genes of each monocyte sub-cluster in Duroc and Meishan pigs. **D** The numbers of genes identified between Duroc and Meishan pigs for each monocyte sub-cluster. **E** The profiles of inter-breed gene expression alterations for the genes showing significantly different changes between Duroc and Meishan pigs in any monocyte sub-clusters

### Heterogeneity and inter-breed differences of αβ and γδ T lymphocyte sub-populations

T lymphocytes can be classified as two major lineages based on their T-cell receptors, including αβ T contributing to adaptive immunity and γδ T mediating both innate and adaptive immunity [46, 58]. Initial clustering identified eight T lymphocyte clusters making up over half of all analyzed PBMCs, which uncover major T clusters such as $CD4^+$ αβ T, $CD8^+$ αβ T and γδ T (Fig. 1; Table S2). To further characterize their heterogeneity, we performed re-clustering analysis on T lymphocytes with finer resolution and identified 21 sub-clusters denoted as T0 - T20, respectively (Fig. 5A). Inspection of known markers indicates that re-clustering analysis identifies additional T cell subsets, such as $CD2^+$ γδ T cells which are embedded within $CD8^+$ T and NK cells in the initial clustering (Fig. 1C, D) and now form distinct clusters (T14, T19) marked with TRDC and CD2 (Fig. 5B and C). The genes that are enriched in each cluster were also identified, with the numbers ranging from 30 to 210 for different clusters (Table S8).

We first examined the αβ T populations which are classified as five $CD4^+$ T (T3, T4, T7, T9, T17) and seven $CD8^+$ T sub-clusters (T2, T5, T8, T10, T11, T13, T15). We examined FOXP3 which marks regulatory T cells (Treg) in human [59], and found it is restrained to the $CD4^+$ T3 cluster (Fig. S6). Interestingly, a small proportion (T18) of $CD4^-CD8^-$ double-negative T cells (DNTCs) were also identified, which are known to be important for inflammation and autoimmunity in human [60]. However, the $CD4^+CD8^+$ DPTCs which form a single cluster in initial analysis are now embedded within cluster T2 which is annotated as $CD4^+$ single-positive predominated (Fig. S7), tend to agree with previous assumption that DPTCs are differentiated from $CD4^+$ single-positive T cells in pigs [61].

Previous studies suggest that porcine γδ T cells can be categorized into two distinct subsets based on the

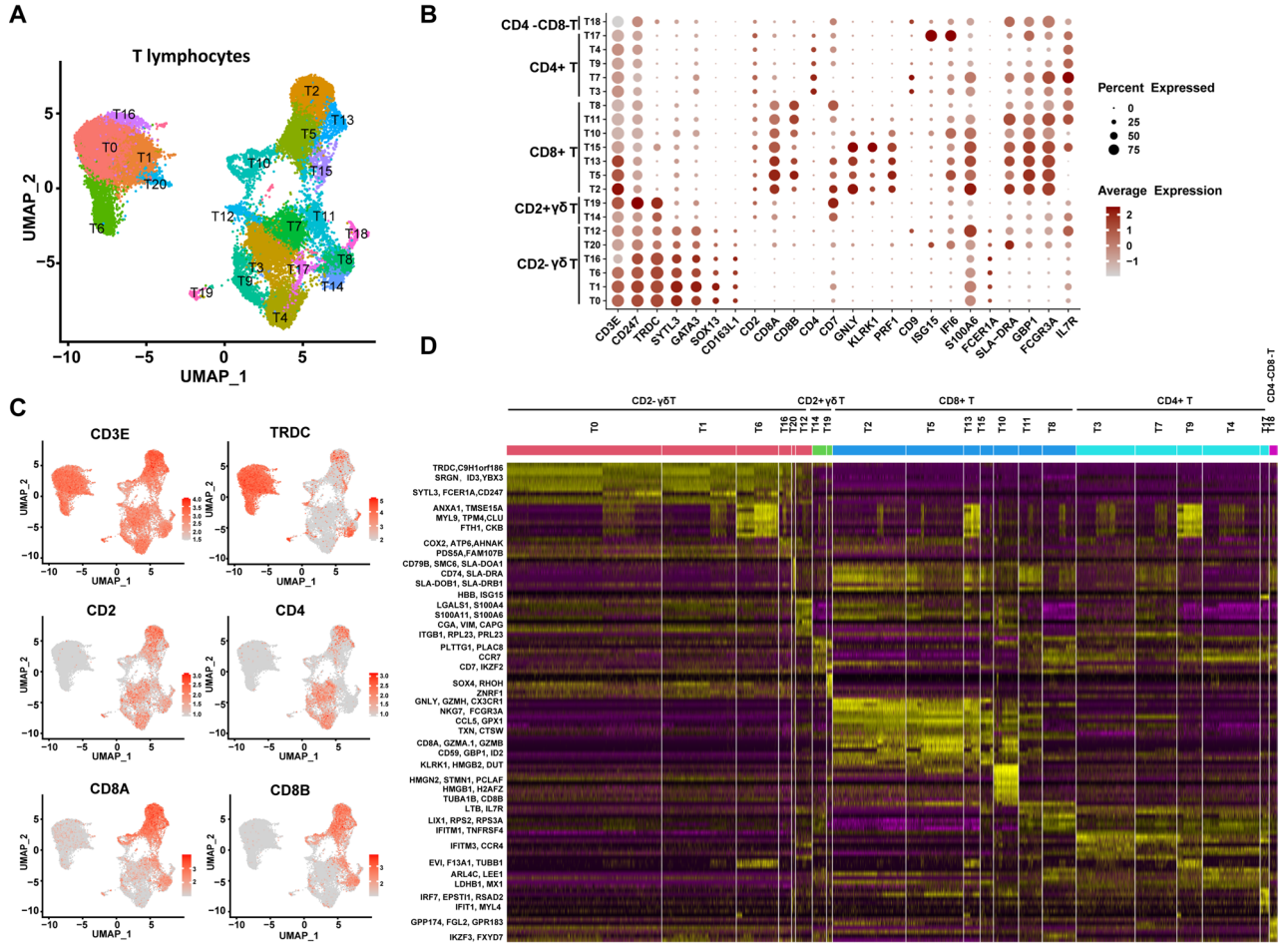


**Fig. 5** Heterogeneity of αβ and γδ T lymphocytes in porcine PBMCs by re-clustering analyses. **A** UMAP visualization of T lymphocyte subsets based on re-clustering analysis. **B** UMAP plots for the expression distribution of 6 representative genes among T subsets. **C** Dot plot for the expression pattern of representative genes among different T lymphocyte subsets. **D** Heatmap for the expression pattern of the top 10 genes with enriched expression in each annotated T lymphocyte subsets. Color indicates the normalized expression value

expression of CD2 [62–64]. Even though initial clustering only identified the CD2$^-$ γδ T subset, re-clustering analysis further uncovered the CD2$^+$ γδ T subtype as clusters T14 and T19 (Fig. 5B-D). Nevertheless, the expression of CD2 in CD2$^+$ γδ T, CD4$^+$ T and CD8$^+$ T cells are sparse, which is in agree with a recent study [34]. As expected, many genes are differentially expressed between CD2$^+$ and CD2$^-$ γδ T subsets. For example, GATA3 and SOX13, which are important for γδ T cell differentiation [65–67], are restricted to CD2$^-$ γδ T sub-clusters (Fig. 5B). We further identified many genes that are enriched in γδ T lymphocytes, such as SYTL3 and CD163L1 (Table S8). Surprisingly, a substantial proportion of cells in cluster T15 express both *CD8A* and *TRDC* but not *CD4* or *CD8B* (Fig. 5B and C). Cluster T15 also highly expresses *KLRK1* (also known as *NKG2D*) which is an activation receptor for T and NK cells [68]. We speculate it may represent a novel subset of T lymphocytes that deserve further studies.

We performed clustering analysis of the 21 T lymphocyte sub-clusters based on their gene expression levels, and demonstrated that all of them are shared by Duroc and Meishan pigs (Fig. 6A). Moreover, most of these sub-clusters are of comparable proportions in Duroc and Meishan pigs, except that the T15 sub-cluster (belongs to CD8$^+$ T) shows significantly higher proportion in Duroc pigs (Fig. 6B). As aforementioned, T15 is a unique sub-cluster expresses high levels of both *CD8A* and *TRDC*, and is marked with *GNLY*, *KLRK1* and *PRF1* which are associated with cytotoxicity (Fig. 5C). For the DEGs identified across T sub-clusters, they usually show highly consistent expression pattern in Duroc and Meishan pigs (Fig. 6C). Subsequently, we identified a total of 421 genes showing altered expression between Duroc and Meishan pigs for these T sub-clusters, with the highest number observed for T5 ($n = 139$) which belongs to CD8$^+$ T cells (Fig. 6D; Table S9). Most sub-clusters show similar trend regarding their inter-breed gene expression pattern, yet the T20 (belongs to CD2- gdT cells) shows notably different patterns (Fig. 6E).

### Heterogeneity and inter-breed differences of B lymphocyte sub-populations

B lymphocytes play key roles for humoral immunity, yet their heterogeneity in pigs remain poorly characterized. Original clustering of all the sequenced PBMCs

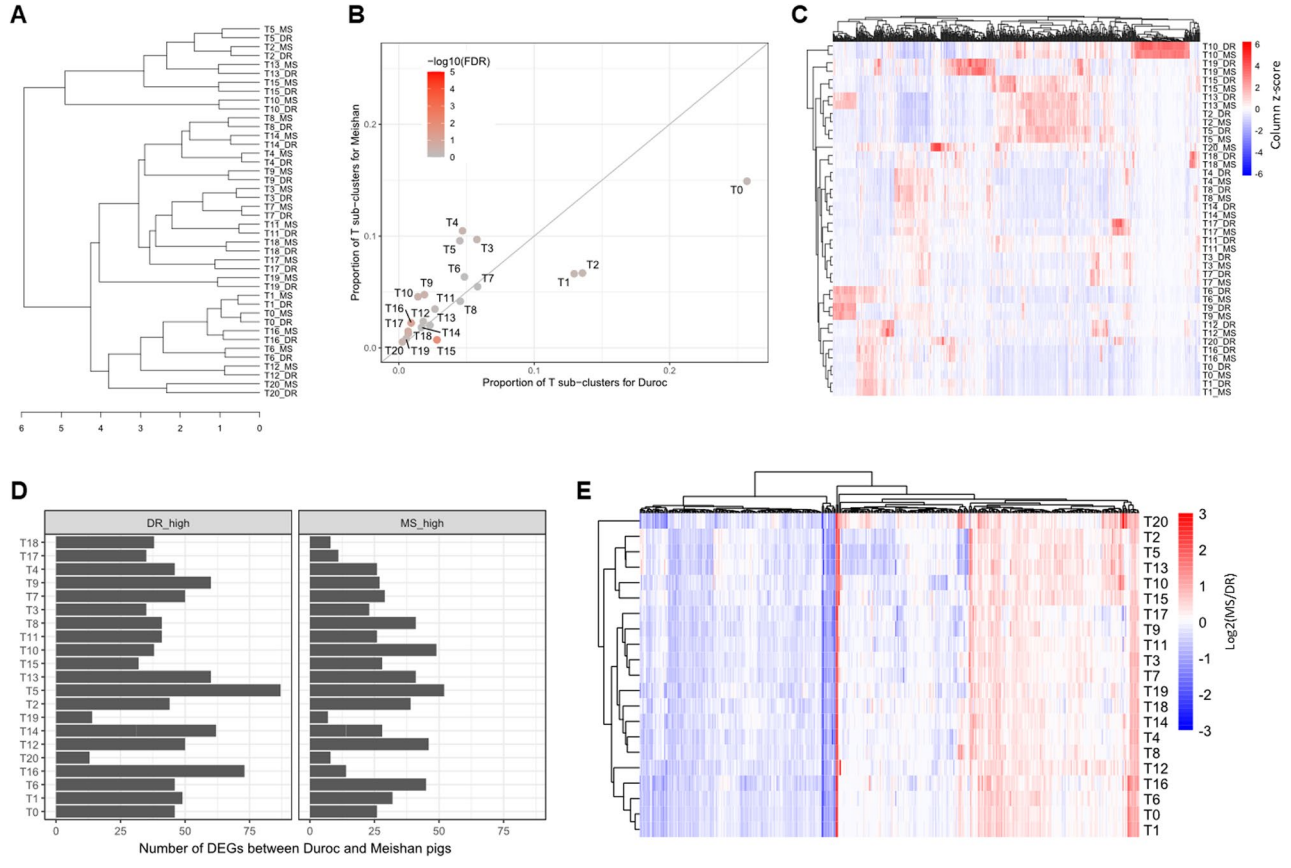


**Fig. 6** Inter-breed differences of cellular proportion and gene expression for T sub-clusters. **A** Hierarchical clustering of T sub-clusters based on their gene expression profiles. **B** Comparison of the cellular proportions of T sub-clusters between Duroc and Meishan pigs. **C** Expression profiles for the marker genes of each T sub-cluster in Duroc and Meishan pigs. **D** The numbers of genes identified between Duroc and Meishan pigs for each T sub-cluster

recovered four clusters of B cells plus one cluster of plasma, which make up 22.2% of all the profiled cells (Fig. 1). Here we further performed re-clustering on these B lymphocytes, which revealed 15 sub-clusters denoted as B0 – B14 (Fig. 7A). Genes overexpressed in each cluster were also identified, which numbers ranging from 28 to 178 (Table S10). Cluster B11 is annotated as plasma according to the expression of *JCHAIN* which is a known marker for plasma cells [69], *HSP90B1* which is involved in the assembly of immunoglobulin [70], and *MZB1* which regulates plasma differentiation [71]. Cluster B13 expresses markers for both B (i.e., CD79B) and T cells (e.g., CD3E, CD8A and CD247) – therefore it represents a mixture of B and T lymphocytes (Fig. 7B-D). The belongings of cluster B10 are ambiguous since it lacks *CD79B* and expresses *HMGB2*, *STMN1*, *DUT* and *TUBB*. Therefore, these three clusters are not further analyzed.

The remaining twelve sub-clusters are characterized as B lymphocytes marked with CD79B expression. They form distinct groups based on known markers and other enriched genes (Table S10). For example, clusters B2, B3, B4, B5 and B9 highly express *FCGR3A*, while B4, B7 and B14 have abundant expression of *MYL9*, *TMSB15A*, *TPM4*, *CKB* and *CLU* (Fig. 7B-D). We demonstrate that *TOX*, *SOX4* and *ID3* are specifically expressed in cluster B9. We also examined *CR2* (also known as *CD21*) which is known to be expressed in mature B cells [72], yet surprisingly its expression in B lymphocytes is sparse (Fig. S8). Interestingly, cluster B12 have abundant expression of several interferon stimulated genes, including *MX1*,

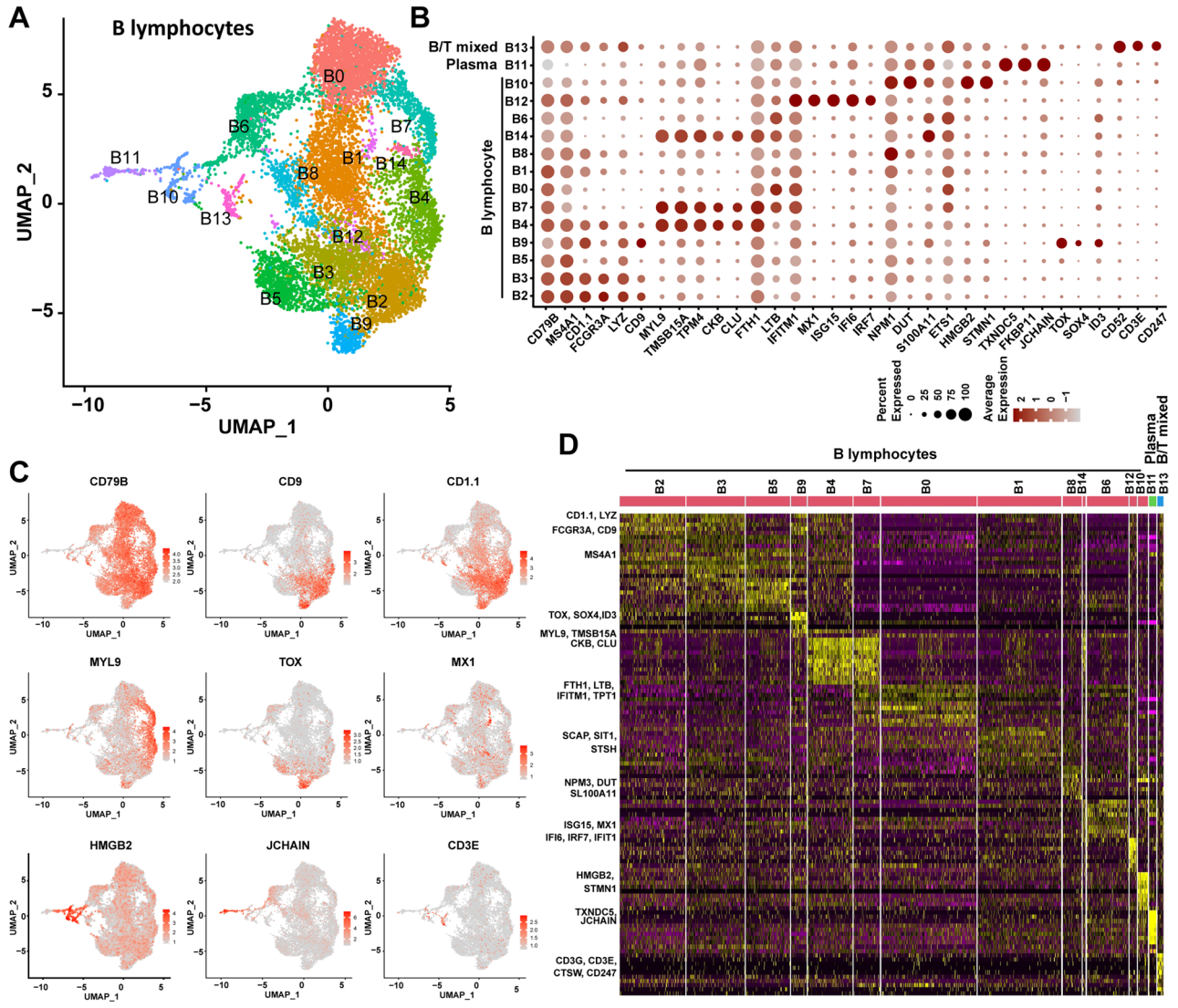


**Fig. 7** Heterogeneity of B lymphocytes in porcine PBMCs revealed by re-clustering analyses. **A** UMAP visualization of B lymphocyte subsets based on re-clustering analysis. **B** UMAP plots for the expression distribution of 6 representative genes among T subsets. **C** Dot plot for the expression pattern of representative genes among different B lymphocyte subsets. **D** Heatmap for the expression pattern of the top 10 genes with enriched expression in each annotated B lymphocyte subsets. Color indicates the normalized expression value

*ISG15*, *IFITM1* and *IRF7* which are important for antiviral response [73] – indicating that this cluster is probably under immune activation (Fig. 7B-D). Notably, re-clustering analysis of T cells also reveals a similar immune-activated cluster (T17) marked with the expression of *MX1*, *ISG15* and *IRF7* (Fig. 5B and D). Together, our data can uncover subpopulations of lymphocytes of distinct lineages or under different immune activation status.

Clustering analysis based on gene expression profiles shows that the thirteen B sub-clusters are conserved in Duroc and Meishan pigs (Fig. 8A). Further comparison shows that while most sub-clusters have similar abundance in Duroc and Meishan pigs, the B2 sub-cluster is of significantly higher proportions in Meishan pigs (Fig. 8B). Of note, the B2 sub-cluster is marked with high expression of CD1.1, FCGR3A, LYZ and CD9 (Fig. 7B). We then examined the expression profiles for the marker genes of each sub-cluster, and found highly similar patterns for Duroc and Meishan pigs (Fig. 7C). Further comparison revealed numerous DEGs between Duroc and Meishan pigs for each sub-cluster, with the numbers ranging from 4 (B14) to 94 (B2) for different sub-clusters (Fig. 8D; Table S11). Interestingly, the B2 cluster is also the only one showing significantly different proportions between Duroc and Meishan pigs (Fig. 8B). At last, we examined the expression alterations for the inter-breed DEGs between Duroc and Meishan pigs (Fig. 8E), and found most sub-clusters show highly similar patterns. Interestingly, the inter-breed gene expression alteration is more evident in B lymphocytes relative to the derived plasma (B11), suggesting the high conservation of the plasma transcriptome across pig breeds.

### Integrative scRNA-seq and scATAC-seq analysis of porcine PBMCs

After uncovering a variety of porcine immune cell sub-populations by scRNA-seq, we further integrated scATAC-seq on matched PBMC samples of Duroc pigs to characterize the chromatin accessibility landscape of each immune cell types. We revealed nineteen distinct cell clusters (Fig. S8), whose structures were similar to those from scRNA-seq data (Fig. 1B) – indicating that single-cell transcriptomic and chromatin accessibility data are largely in consistency. We then assigned the cell types for the cells profiled by scATAC-seq using scRNA-seq-based cell labelling as reference (Fig. 9A).

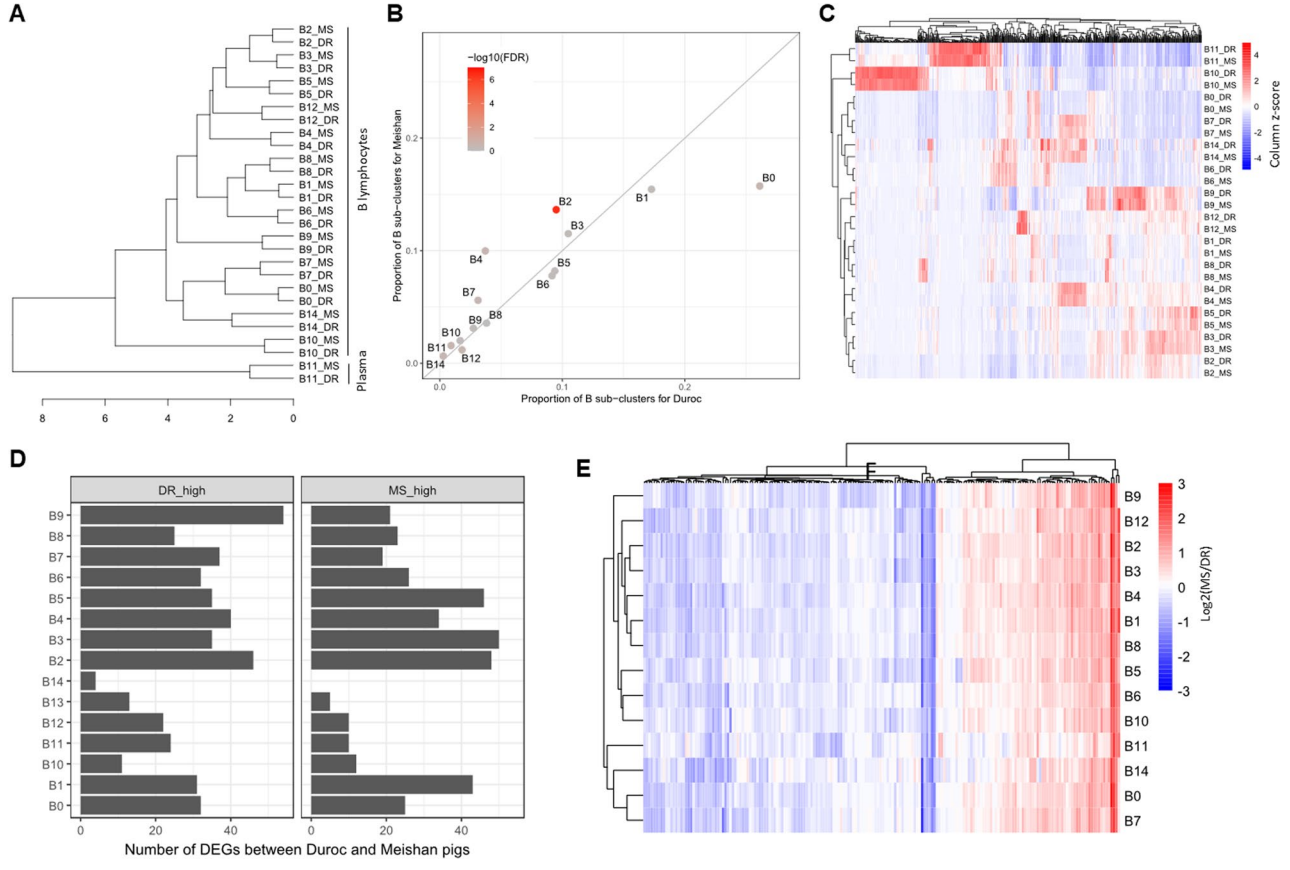


**Fig. 8** Inter-breed differences of cellular proportion and gene expression for B sub-clusters. **A** Hierarchical clustering of B sub-clusters based on their gene expression profiles. **B** Comparison of the cellular proportions of B sub-clusters between Duroc and Meishan pigs. **C** Expression profiles for the marker genes of each B sub-cluster in Duroc and Meishan pigs. **D** The numbers of genes identified between Duroc and Meishan pigs for each B sub-cluster

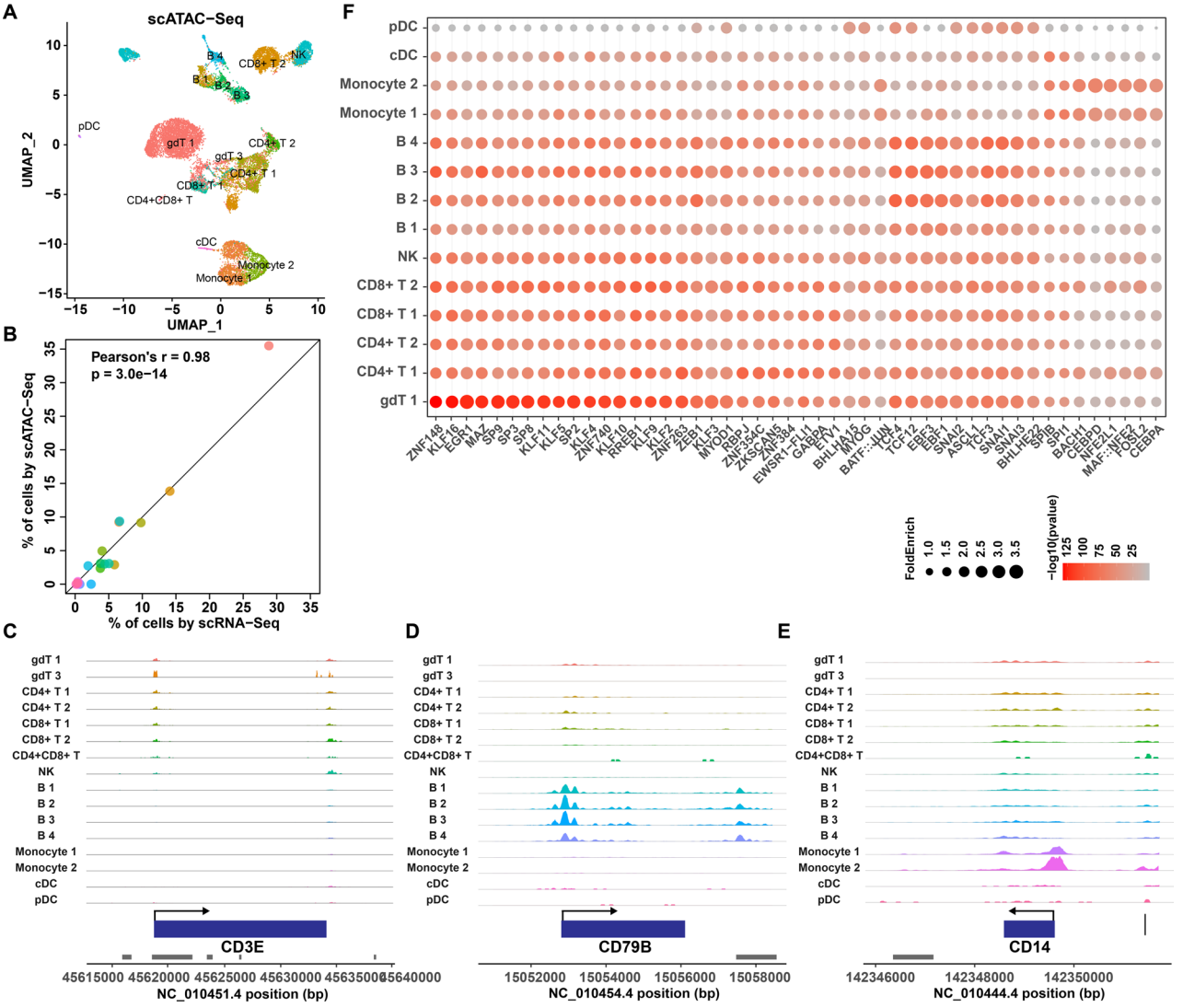


**Fig. 9** Integration of scRNA-Seq and scATAC-Seq data for porcine PBMCs. **A** UMAP visualization of porcine PBMCs based on scATAC-Seq data with scRNA-Seq clustering results as reference for matching. **B** Scatter plot shows that the proportions of cell clusters by scRNA-Seq and scATAC-Seq data are highly correlated. **C-E** Demo tracks for the chromatin accessibility status of CD3E (**C**), CD79B (**D**) and CD14 (**E**) among different cell clusters. The arrows indicate the direction for transcription. **F** Representative motifs enriched in different clusters

The majority (16 out of 20) of annotated cell types can be detected by scATAC-seq, with four small clusters (γδ T 2, $CD8^+$ T3, plasma and platelet) missed likely due to their low proportions in PBMCs. We further compared the percentages of each cell types as inferred by scRNA-seq and scATAC-seq and confirmed that they are highly correlated (Fig. 9B. Pearson's $r = 0.98$, $p = 3.0e\text{-}14$) –supporting the overall consistency of the scRNA-seq and scATAC-seq data. Examination of several canonical markers (i.e., CD3E, CD79B and CD14) confirmed that the chromatin accessibility of these marker genes matches their expression patterns among cell clusters. For example, the promoter region of *CD3E* is only accessible in T lymphocyte clusters (Fig. 6C), *CD79B* only in B lymphocytes (Fig. 9D), and *CD14* only in monocytes (Fig. 9E).

To uncover the core transcription factors for each immune cell types, we further performed motif enrichment analysis for the peaks specific for each cluster. The numbers of significantly enriched motifs range from 83 to 633 for different cell clusters (Table S12, Fig. S10), with a remarkable number of motifs are most highly enriched in the γδ T 1 cluster (Fig. 6F). Notably, motifs for several transcription factors known to be important for the development of specific immune lineages, such as EBF1 for B lymphocyte [74, 75], SPI1 (also known as PU.1) for monocyte [76], are overrepresented in the corresponding cell clusters (Fig. 9F, S10). Among the motifs enriched in γδ T 1 cluster, several are for transcription factors

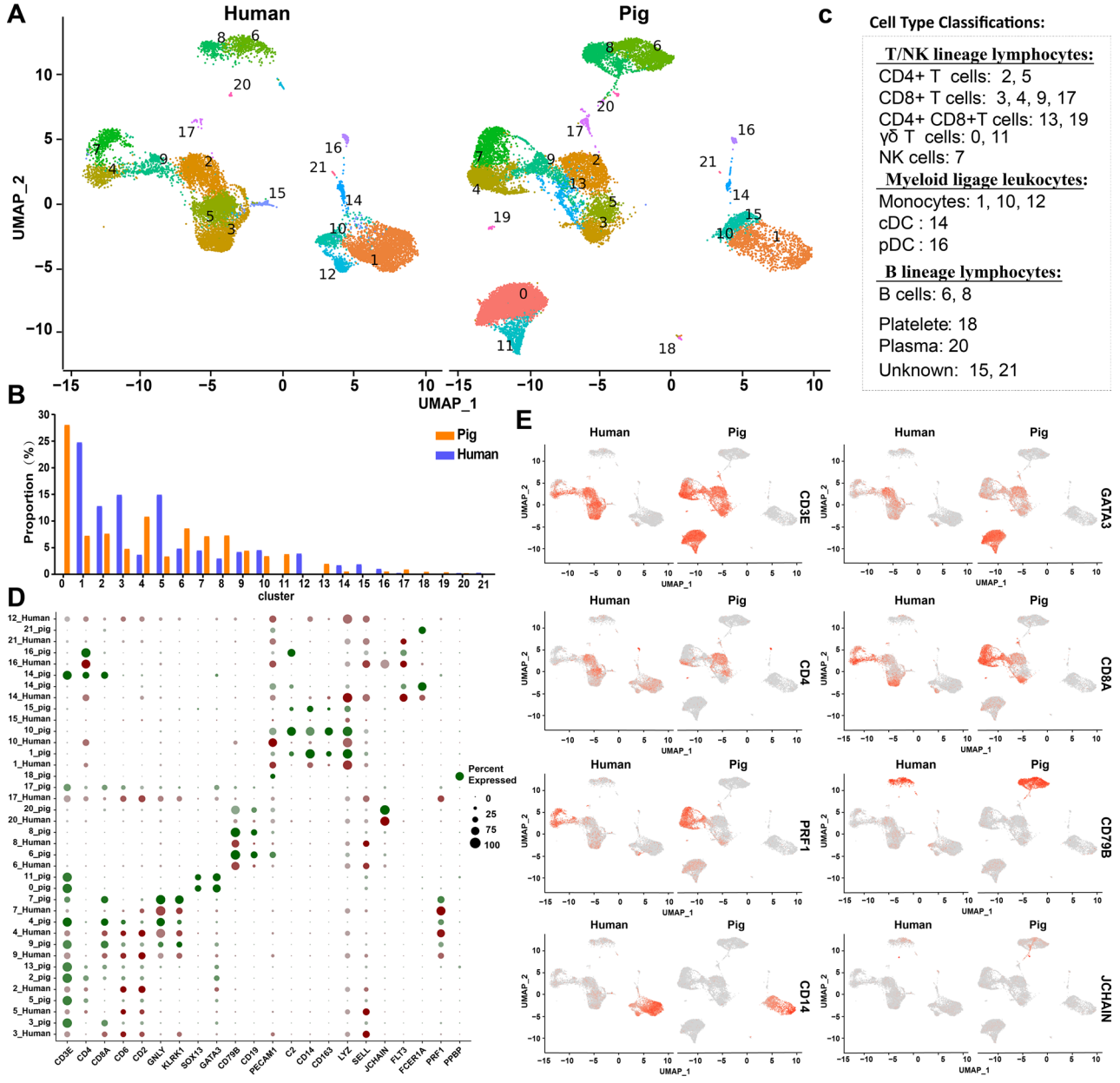


**Fig. 10** Cross-species integration of single-cell transcriptomic data for human and porcine PBMC samples. **A** UMAP visualization of the single-cell transcriptomic data for human and porcine PBMCs. **B** Proportions of each cell cluster in different porcine and human PBMC samples. **C** The annotation of each cluster indicated in A and B. **D** Expression pattern of eight representative genes across annotated cell clusters for human and porcine PBMC samples. **E** Expression abundance of representative genes in each cell cluster between Human and pigs. The expression values in pigs are indicated by green color, and in human by red color

important for γδ T development, particularly KLFs which can regulate the trafficking and homeostasis of γδ T lymphocytes [77, 78]. Together, our scATAC-seq data are useful in dissecting the heterogeneity of porcine immune cells in PBMCs and predicting the transcription factors associated with each immune cell subsets.

### Integrative analysis of porcine and human scRNA-seq datasets

To analyze the potential difference of the immune cell heterogeneity between pig and human, we compared our scRNA-seq data against matched dataset for human PBMCs. UMAP visualization on the pooled datasets revealed 22 cell clusters (Fig. 10A). Except for five clusters (0, 11, 13, 19, 18) absent in human and one cluster (12) absent in pigs, all other clusters are presented in both species with comparable proportion (Fig. 10B; Table S10).

Based on known cell markers, all the major cell populations are annotated including T, B, NK, myeloid, DC and platelet-like clusters (Fig. 7C-E), yet two clusters (15, 21) were not annotated likely due to their low proportions. The major T sub-clusters such as $CD4^+$ αβ T, $CD8^+$ αβ T, $CD4^+CD8^+$ DPTCs and γδ T were further annotated (Fig. 10C). Interestingly, the $CD4^+CD8^+$ DPTCs and γδ T cells are absent in human samples, notably γδ T cells are of particularly high proportion (31.6%) in pig PBMCs (Fig. 10B; Table S13). On contrast, myeloid show remarkably higher proportion in human PBMCs (32.9% vs. 10.5%) (Fig. 7B; Table S10). Surprisingly, human possess one additional monocyte cluster (cluster 12) relative to pig, which makes up 3.8% of human PBMCs (Table S13). This cluster expresses not only common myeloid markers (e.g., *CD14* and *LYZ*), but also some genes (e.g. *CD2*, *CD6*, *GNLY*, *KLRK1*, *PRF1*) that are low in other myeloid sub-clusters (Fig. 10E, S11)–inspection of these markers suggest that this cluster matches the "Mono4" sub-cluster reported by previous studies in human blood [30]. Further, we found that some genes show different expression abundance in matched clusters between human and pig (Fig. 7E). Together, our results demonstrate that while major immune cell lineages and the corresponding marks match between human and pig, several unshared cell populations ("Mono4" in human, $CD4^+CD8^+$ DPTCs and γδ T in pig) may deserve further studies.

## Discussion

The domestic pig serves as an advantageous model for immunology and biomedical studies [4]. Single-cell transcriptomic and chromatin accessibility profiling enables comprehensive characterization of the immune cell heterogeneity in humans [26, 29, 79]. Unfortunately, single-cell resolution studies on porcine immune systems are still rare. While one recent study applied scRNA-seq to characterize porcine immunity [34] - the analyzed PBMC samples are from crossbred pigs which precluded further investigation of the inter-breed immune trait variations. Aiming at finer resolution annotation of the immune cell populations at both transcriptomic and regulatory levels and revealing the molecular mechanisms underlying the inter-breed immune variations, we present the first comprehensive single-cell transcriptomic maps of the PBMCs of Meishan and Duroc pigs together with single-cell chromatin maps of matched Duroc samples.

In this study, we profiled a total of 63,710 single-cell transcriptomes for porcine PBMCs, which enable comprehensive annotation of the porcine immune cell heterogeneity at unprecedented resolution. After pooling all the scRNA-seq data together, we uncovered twenty distinct cell clusters, with all clusters uncovered in both Duroc and Meishan samples - suggesting that the immune cell subsets match well across breeds. All major immune cell types, including αβ T, γδ T, B, myeloid, NK and DC, can be annotated by our data. Notably, the γδ T lymphocytes make up almost one-fifth of all the analyzed PBMCs, which is much higher than in humans and mice [13, 80]. Interestingly, the γδ T proportion ranges dramatically between 10.7% and 46.7% among our samples and is estimated as 9.2% based on recently published data for cross-breed porcine PBMCs [34] - suggesting extraordinary variations of the γδ T proportions among breeds and individuals. The molecular mechanism underlying highly abundant γδ T in pigs and variable proportions across breeds and individuals is still unclear. However, given that the analyzed samples in our study are of the same breed and matched age – therefore the between-individual variations of γδ T proportions are more likely due to specific environmental or physiology factors.

Apart from uncovering major immune cell populations, re-clustering analyses with finer resolution succeed in identifying almost fifty sub-populations for the three major immune lineages, including T, B and myeloid cells. The re-clustering analyses provide more details about the heterogeneity of porcine immunity, which are overlooked in the initial clustering analysis. For example, re-clustering analyses uncover the $CD2^+$ γδ T subsets, yet the corresponding cells are embedded within $CD8^+$ αβ clusters based on initial clustering. Re-clustering also confirms several other minority sub-populations, such as the $CD4^-$ $CD8^-$ DNTCs which are known to be important for inflammation, autoimmunity in human [60] and immune homeostatic milieu [81], and T, B and myeloid cells expressing MX1 and ISG15 which tend to represent the activated sub-populations. Importantly, numerous putative cell markers are also identified, including some novel ones which may facilitate further experimental studies of corresponding immune cell sub-populations. In summary, our single-cell transcriptomic data enable comprehensive annotation of the cell sub-populations and corresponding marker genes for porcine PBMCs.

It has been well recognized that immune traits, which are critical for animal health and pathogen resistance, vary remarkably among porcine breeds [17, 19], yet the underlying molecular mechanism remains largely unresolved. Single-cell resolution profiling of the transcriptomes for two distinct breeds, including Duroc and Meishan with the latter of relatively high immune capacity, provides the opportunity to address this question. We demonstrate that the immune cell subsets with remarkable altered proportions across breeds are usually those critical for innate immunity, including monocytes which are overrepresented in Meishan pigs, and NK cell that are enriched in Duroc pigs. It agrees with previous observation that Meishan pigs have higher monocyte counts in blood [17]. Our data also enable direct comparison of the transcriptomes of each matched immune cell type across

breeds. Focusing on monocytes and γδ T lymphocytes, we found that genes overexpressed in Meishan pigs are highly associated with immune response-related functions, while those overexpressed in Duroc pigs are less associated with immune response and show enrichment of the reversed function "negative regulation of immune system process". Together, innate immunity seems to be critical for the inter-breed immune variations, and both the cellular compositions and gene expression patterns of counterpart cell types are associated with the inter-breed immune variations.

Taking advantage of the re-clustering results, we also attempted to compare if specific sub-clusters for B, T and monocytes exist in only Duroc or Meishan pigs. We found that all the sub-clusters are shared by Duroc and Meishan pigs, suggesting that the immune cell populations are conserved across pig breeds. This is not surprising given that there has only been 9000–10,000 years since the domestication of pigs. Moreover, the relative proportions of most sub-populations (except for 2 of the 14 monocyte sub-clusters, 1 of the 20 T sub-clusters, and 1 of the 13 B sub-clusters) are comparable between Duroc and Meishan pigs. Further comparison identified hundreds of genes showing altered expression between Duroc and Meishan pigs for these sub-clusters. We found that the inter-breed gene expression differences are highly similar for the sub-clusters of the same major immune cells. Together, it suggests the inter-breed differences of immune cellular compositions and gene expression mainly represents for major clusters instead of further differentiated sub-clusters, indicating such differences are usually established before the differentiation of the immune cell subsets.

We also applied scATAC-seq to generate 21,855 single-cell chromatin accessibility maps for matched PBMC samples of Duroc pigs, aiming at characterizing the chromatin accessibility landscape and uncover core transcription factors for each immune cell population. Integrative analysis of scRNA-seq and scATAC-seq data suggests that the motifs for several transcription factors critical for the development of distinct immune lineages are enriched in the accessible peaks for corresponding cell clusters, such as EBF1 for B lymphocyte [74], SPI1 for monocyte and macrophage [76], and KLF factors for γδ T lymphocyte [77, 78]. Apart from them, motifs for a dozen of other transcription factors are also significantly enriched in specific clusters, which may deserve further investigation. These results show that integrating of scRNA-seq and scATAC-seq data are useful in dissecting the heterogeneity of porcine immune cells and identifying the transcription factors associated with each immune cell subsets.

Integration of matched scRNA-seq datasets for human and porcine PBMCs demonstrates that while most immune cell lineages and the corresponding marks match between species, this agrees with one previous study [34]. Interestingly, our analysis further reveals that several cell populations that are only presented in one species, including $CD4^+CD8^+$ DPTCs and γδ T in pig, and "Mono4" in human. It has long been known that γδ T lymphocytes are abundant in pigs and rare in humans [34, 63], yet the complete loss in human tend to suggest that the cell markers of this lineage also differ between human and pig. Regarding $CD4^+CD8^+$ DPTCs, previous studies also suggest higher abundance in pigs relative to humans and mice [82]. Notably, their abundance are associated with health status and age, which increase with age in humans [83], and coincide with thymic involution in cynomolgus monkeys [84]. The "Mono4" cluster in human PBMCs expressed cytotoxic gene signature (*PRF1* and *GNLY*) and resembles previously reported "natural killer dendritic cells" [30], however the absence of "Mono4" cluster in pigs is not reported before and the mechanism remains unclear. Collectively, these unshared immune cell sub-populations between human and pigs may deserve further studies in the future.

To our knowledge, this study represents the most comprehensive single-cell transcriptomic and regulatory profiling of porcine PBMCs from two distinct breeds at unprecedented resolution. This study improves our understanding about the immune heterogeneity and inter-breed immune trait variations in pigs. We also expect the cell sub-populations, immune markers and core regulators identified in this study would be valuable in facilitating future biomedical studies about human immunology and organ xenotransplantation.

## Supplementary Information

The online version contains supplementary material available at https://doi.org/10.1186/s12864-026-12854-0.

Supplementary Material 1. Supplementary tables: Additional file 1: Table S1. Data resources. Additional file 2: Table S2. Cluster fraction. Additional file 3: Table S3. Enriched genes in each cluster. Additional file 4: Table S4. GO enrichment for major clusters. Additional file 5: Table S5. Inter-breed DEGs. Additional file 6: Table S6. Myeloid subset markers. Additional file 7: Table S7. Myeloid subset breed-specific DEGs. Additional file 8: Table S8. T subset markers. Additional file 9: Table S9. T subset breed-specific DEGs. Additional file 10: Table S10. B subset markers. Additional file 11: Table S11. B subset breed-specific DEGs. Additional file 12: Table S12. Enriched motifs for DA peaks. Additional file 13: Table S13. Proportions of each cell cluster in different porcine and Human PBMC samples annotated by scRNA-seq. Figs. S1 to S11.

#### Acknowledgements

The authors thank all the staff involved in the pigs' care and feeding. This study utilized the computational resource of the Yangzhou University College of Veterinary Medicine High-Performance Computing Cluster.

#### Authors' contributions

W.B., and H.F. conceived and designed the study. H.F., and C.X. performed animal work and prepared biological samples. M.S., C.D. and H.F. analyzed the scRNA-seq and scATAC-seq data. M.S., and H.F. drafted and wrote the

manuscript. H.W., Y.W., Z.W., B.Z., C.C., S.S., and W.B. revised the manuscript. All authors read and approved the final version of the manuscript.

**Funding**
This work was supported by National Key Research and Development Program of China (2023YFF1000900, 2023ZD0404403-03), National Natural Science Foundation of China (32502857) and Jiangsu Basic Science (Natural Science) Research Project of Higher Education Institutions (24KJD230003).

**Data availability**
Sequence data that support the findings of this study have been deposited in the Gene Expression Omnibus (GEO) database (https://www.ncbi.nlm.nih.gov/geo/) under accession GSE196044. There are no restrictions on data availability or use. All other data generated and analyzed during this study are included in this published article and its supplementary information files.

## Declarations

**Ethics approval and consent to participate**
All experiments were approved by the Animal Care and Use Committee of Yangzhou University (license approval number: SYXK (Su) 2021-0026). Before the project began, informed consent was obtained from all relevant personnel. The 10x multiome data of human PBMCs was downloaded from the 10x genomics website: https://support.10xgenomics.com/single-cell-multiome-atac-gex/datasets/1.0.0/pbmc_granulocyte_sorted_10k.

**Consent for publication**
All authors have read the journal's position on issues involved in ethical publication, and all authors have approved the final version of the manuscript.

**Competing interests**
The authors declare no competing interests.

**Author details**
[1]Key Laboratory for Animal Genetics, Breeding, Reproduction and Molecular Design, College of Animal Science and Technology, Yangzhou University, Yangzhou, Jiangsu 225009, China
[2]Institute of Comparative Medicine, College of Veterinary Medicine, Yangzhou University, Yangzhou, Jiangsu 225009, China
[3]School of Basic Medicine, Shenzhen University Health Science Center, Shenzhen, Guangdong 518060, China
[4]National Clinical Research Center for Metabolic Diseases, Key Laboratory of Diabetes Immunology, Ministry of Education, and Department of Metabolism and Endocrinology, The Second Xiangya Hospital of Central South University, Changsha, Hunan 410011, China
[5]Department of Pediatrics, Aflac Cancer and Blood Disorders Center, Winship Cancer Institute, Children's Healthcare of Atlanta, Emory University, Atlanta, GA 30322, USA

Received: 21 November 2025 / Accepted: 8 April 2026
Published online: 25 April 2026

**References**

1. Almeida FF, Leal MC, Franca LR. Testis morphometry, duration of spermatogenesis, and spermatogenic efficiency in the wild boar (*Sus scrofa scrofa*). Biol Reprod. 2006;75(5):792–9.
2. Meurens F, Summerfield A, Nauwynck H, Saif L, Gerdts V. The pig: a model for human infectious diseases. Trends Microbiol. 2012;20(1):50–7.
3. Litten-Brown JC, Corson AM, Clarke L. Porcine models for the metabolic syndrome, digestive and bone disorders: a general overview. Animal. 2010;4(6):899–920.
4. Pabst R. The pig as a model for immunology research. Cell Tissue Res. 2020;380(2):287–304.
5. Fairbairn L, Kapetanovic R, Sester DP, Hume DA. The mononuclear phagocyte system of the pig as a model for understanding human innate immunity and disease. J Leukoc Biol. 2011;89(6):855–71.
6. Summerfield A, McCullough KC. The porcine dendritic cell family. Dev Comp Immunol. 2009;33(3):299–309.
7. Bailey M, Christoforidou Z, Lewis MC. The evolutionary basis for differences between the immune systems of man, mouse, pig and ruminants. Vet Immunol Immunopathol. 2013;152(1–2):13–9.
8. Dawson HD, Loveland JE, Pascal G, Gilbert JG, Uenishi H, Mann KM, Sang Y, Zhang J, Carvalho-Silva D, Hunt T, et al. Structural and functional annotation of the porcine immunome. BMC Genomics. 2013;14:332.
9. Bonneville M, O'Brien RL, Born WK. Gammadelta t cell effector functions: a blend of innate programming and acquired plasticity. Nat Rev Immunol. 2010;10(7):467–78.
10. Pang DJ, Neves JF, Sumaria N, Pennington DJ. Understanding the complexity of gammadelta T-cell subsets in mouse and human. Immunology. 2012;136(3):283–90.
11. Sullivan ZA, Khoury-Hanold W, Lim J, Smillie C, Biton M, Reis BS, et al. : γδ t cells regulate the intestinal response to nutrient sensing. Science. 2021;371(6535):eaba8310.
12. Born W, Cady C, Jones-Carson J, Mukasa A, Lahn M, O'Brien R. Immunoregulatory functions of gd T cells. Adv Immunol. 1999;71:77–144.
13. Takamatsu HH, Denyer MS, Stirling C, Cox S, Aggarwal N, Dash P, et al. Porcine gammadelta t cells: possible roles on the innate and adaptive immune responses following virus infection. Vet Immunol Immunopathol. 2006;112(1–2):49–61.
14. Pizzolato G, Kaminski H, Tosolini M, Franchini DM, Pont F, Martins F, Valle C, Labourdette D, Cadot S, Quillet-Mary A, et al. Single-cell RNA sequencing unveils the shared and the distinct cytotoxic hallmarks of human TCRVdelta1 and TCRVdelta2 gammadelta T lymphocytes. Proc Natl Acad Sci U S A. 2019;116(24):11906–15.
15. Murtaugh MP, Johnson CR, Xiao Z, Scamurra RW, Zhou Y. Species specialization in cytokine biology: is interleukin-4 central to the T(H)1-T(H)2 paradigm in swine? Dev Comp Immunol. 2009;33(3):344–52.
16. Bovo S, Ribani A, Munoz M, Alves E, Araujo JP, Bozzi R, Candek-Potokar M, Charneca R, Di Palma F, Etherington G, et al. Whole-genome sequencing of European autochthonous and commercial pig breeds allows the detection of signatures of selection for adaptation of genetic resources to different breeding and production systems. Genet Sel Evol. 2020;52(1):33.
17. Clapperton M, Bishop SC, Glass EJ. Innate immune traits differ between Meishan and Large White pigs. Vet Immunol Immunopathol. 2005;104(3–4):131–44.
18. Halbur PG, Rothschild MF, Thacker BJ, Meng X-J, Paul PS. Differences in susceptibility of Duroc, Hampshire, and Meishan pigs to infection with a high virulence strain (VR2385) of porcine reproductive and respiratory syndrome virus (PRRSV). J Anim Breed Genet. 1998;115:181–9.
19. Sutherland MA, Rodriguez-Zas SL, Ellis M, Salak-Johnson JL. Breed and age affect baseline immune traits, cortisol, and performance in growing pigs. J Anim Sci. 2005;83(9):2087–95.
20. Wei R, Trus I, Yang B, Huang L, Nauwynck HJ. Breed differences in PCV2 uptake and disintegration in porcine monocytes. Viruses. 2018;10(10):562.
21. Pei Y, Lin C, Li H, Feng Z. Genetic background influences pig responses to porcine reproductive and respiratory syndrome virus. Front Vet Sci. 2023;10:1289570.
22. Duchet-Suchaux MF, Bertin AM, Menanteau PS. Susceptibility of Chinese Meishan and European large white pigs to enterotoxigenic *Escherichia coli* strains bearing colonization factor K88, 987P, K99, or F41. Am J Vet Res. 1991;52(1):40–4.
23. Reiner G, Melchinger E, Kramarova M, Pfaff E, Buttner M, Saalmuller A, Geldermann H. Detection of quantitative trait loci for resistance/susceptibility to pseudorabies virus in swine. J Gen Virol. 2002;83(Pt 1):167–72.
24. Reiner G, Eckert J, Peischl T, Bochert S, Jakel T, Mackenstedt U, et al. Variation in clinical and parasitological traits in Pietrain and Meishan pigs infected with *Sarcocystis miescheriana*. Vet Parasitol. 2002;106(2):99–113.
25. Lu X, Fu WX, Luo YR, Ding XD, Zhou JP, Liu Y, Liu JF, Zhang Q. Genome-wide association study for T lymphocyte subpopulations in swine. BMC Genomics. 2012;13:488.
26. Papalexi E, Satija R. Single-cell RNA sequencing to explore immune cell heterogeneity. Nat Rev Immunol. 2018;18(1):35–45.
27. Stubbington MJT, Rozenblatt-Rosen O, Regev A, Teichmann SA. Single-cell transcriptomics to explore the immune system in health and disease. Science. 2017;358(6359):58–63.
28. Satpathy AT, Granja JM, Yost KE, Qi Y, Meschi F, McDermott GP, Olsen BN, Mumbach MR, Pierce SE, Corces MR, et al. Massively parallel single-cell chromatin landscapes of human immune cell development and intratumoral T cell exhaustion. Nat Biotechnol. 2019;37(8):925–36.

29. Ranzoni AM, Tangherloni A, Berest I, Riva SG, Myers B, Strzelecka PM, Xu J, Panada E, Mohorianu I, Zaugg JB, et al. Integrative Single-Cell RNA-Seq and ATAC-Seq Analysis of Human Developmental Hematopoiesis. Cell Stem Cell. 2021;28(3):472–e487477.
30. Villani AC, Satija R, Reynolds G, Sarkizova S, Shekhar K, Fletcher J, Griesbeck M, Butler A, Zheng S, Lazo S, et al. Single-cell RNA-seq reveals new types of human blood dendritic cells, monocytes, and progenitors. Science. 2017;356(6335):eaah4573.
31. Zhang JY, Wang XM, Xing X, Xu Z, Zhang C, Song JW, Fan X, Xia P, Fu JL, Wang SY, et al. Single-cell landscape of immunological responses in patients with COVID-19. Nat Immunol. 2020;21(9):1107–18.
32. Zhu L, Yang P, Zhao Y, Zhuang Z, Wang Z, Song R, Zhang J, Liu C, Gao Q, Xu Q, et al. Single-Cell Sequencing of Peripheral Mononuclear Cells Reveals Distinct Immune Response Landscapes of COVID-19 and Influenza Patients. Immunity. 2020;53(3):685–e696683.
33. Zhi C, Shi X, Chen S, Cai Z, Jiang X. Single-cell transcriptome analysis revealed critical causative candidates for down syndrome-related lung diseases. J Genet Genomics . 2026;53(1):75-86. https://doi.org/10.1016/j.jgg.2025.05.009.
34. Herrera-Uribe J, Wiarda JE, Sivasankaran SK, Daharsh L, Liu H, Byrne KA, Smith TPL, Lunney JK, Loving CL, Tuggle CK. Reference Transcriptomes of Porcine Peripheral Immune Cells Created Through Bulk and Single-Cell RNA Sequencing. Front Genet. 2021;12:689406.
35. Wolock SL, Lopez R, Klein AM. Scrublet: Computational Identification of Cell Doublets in Single-Cell Transcriptomic Data. Cell Syst. 2019;8(4):281–91. e289.
36. Stuart T, Butler A, Hoffman P, Hafemeister C, Papalexi E, Mauck WM 3rd, Hao Y, Stoeckius M, Smibert P, Satija R. Comprehensive Integration of Single-Cell Data. Cell. 2019;177(7):1888–902. e1821.
37. Drokhlyansky E, Smillie CS, Van Wittenberghe N, Ericsson M, Griffin GK, Eraslan G, Dionne D, Cuoco MS, Goder-Reiser MN, Sharova T, et al. The Human and Mouse Enteric Nervous System at Single-Cell Resolution. Cell. 2020;182(6):1606–e16221623.
38. Phipson B, Sim CB, Porrello ER, Hewitt AW, Powell J, Oshlack A. Propeller: testing for differences in cell type proportions in single cell data. Bioinformatics. 2022;38(20):4720–6.
39. Du C, Fan H, Jiang J, Yang J, Chen S, Vorobyeva NE, Zhu C, Mao L, Li C, Li Y, et al. Multiomic analyses on the contribution of transposable elements to the cis-regulatory landscape of different types of immune cells. BMC Genomics. 2025;26(1):1077.
40. Stuart T, Srivastava A, Madad S, Lareau CA, Satija R. Single-cell chromatin state analysis with signac. Nat Methods. 2021;18(11):1333–41.
41. Cusanovich DA, Daza R, Adey A, Pliner HA, Christiansen L, Gunderson KL, Steemers FJ, Trapnell C, Shendure J. Multiplex single cell profiling of chromatin accessibility by combinatorial cellular indexing. Sci (New York NY). 2015;348(6237):910–4.
42. Zhang Y, Liu T, Meyer CA, Eeckhoute J, Johnson DS, Bernstein BE, Nusbaum C, Myers RM, Brown M, Li W, et al. Model-based analysis of ChIP-Seq (MACS). Genome Biol. 2008;9(9):R137.
43. Yu G, Wang L-G, He Q-Y. ChIPseeker: an R/Bioconductor package for ChIP peak annotation, comparison and visualization. Bioinf (Oxford England). 2015;31(14):2382–3.
44. Huang da W, Sherman BT, Lempicki RA. Systematic and integrative analysis of large gene lists using DAVID bioinformatics resources. Nat Protoc. 2009;4(1):44–57.
45. Fornes O, Castro-Mondragon JA, Khan A, van der Lee R, Zhang X, Richmond PA, Modi BP, Correard S, Gheorghe M, Baranasic D, et al. JASPAR 2020: update of the open-access database of transcription factor binding profiles. Nucleic Acids Res. 2020;48(D1):D87–92.
46. Gerner W, Kaser T, Saalmuller A. Porcine T lymphocytes and NK cells–an update. Dev Comp Immunol. 2009;33(3):310–20.
47. Charerntantanakul W, Roth JA. Biology of porcine T lymphocytes. Anim Health Res Rev. 2007;7(1–2):81–96.
48. Ezquerra A, Revilla C, Alvarez B, Perez C, Alonso F, Dominguez J. Porcine myelomonocytic markers and cell populations. Dev Comp Immunol. 2009;33(3):284–98.
49. Sinkora M, Butler JE. The ontogeny of the porcine immune system. Dev Comp Immunol. 2009;33(3):273–83.
50. Nascimbeni M, Shin EC, Chiriboga L, Kleiner DE, Rehermann B. Peripheral CD4(+)CD8(+) T cells are differentiated effector memory cells with antiviral functions. Blood. 2004;104(2):478–86.
51. Okutani M, Tsukahara T, Kato Y, Fukuta K, Inoue R. Gene expression profiles of CD4/CD8 double-positive T cells in porcine peripheral blood. Anim Sci J. 2018;89(7):979–87.
52. Ziegler-Heitbrock L. The CD14 + CD16+ blood monocytes: their role in infection and inflammation. J Leukoc Biol. 2007;81(3):584–92.
53. Chamorro S, Revilla C, Alvarez B, Alonso F, Ezquerra A, Dominguez J. Phenotypic and functional heterogeneity of porcine blood monocytes and its relation with maturation. Immunology. 2005;114(1):63–71.
54. Gillette MA, Mani DR, Uschnig C, Pellé KG, Madrid L, Acácio S, Lanaspa M, Alonso P, Valim C, Carr SA, et al. Biomarkers to Distinguish Bacterial From Viral Pediatric Clinical Pneumonia in a Malaria-Endemic Setting. Clin Infect Dis. 2021;73(11):e3939–48.
55. Balestrieri ML, Balestrieri A, Mancini FP, Napoli C. Understanding the immunoangiostatic CXC chemokine network. Cardiovasc Res. 2008;78(2):250–6.
56. Mossel DM, Moganti K, Riabov V, Weiss C, Kopf S, Cordero J, Dobreva G, Rots MG, Kluter H, Harmsen MC, et al. Epigenetic Regulation of S100A9 and S100A12 Expression in Monocyte-Macrophage System in Hyperglycemic Conditions. Front Immunol. 2020;11:1071.
57. Hu Y, Hu Y, Xiao Y, Wen F, Zhang S, Liang D, Su L, Deng Y, Luo J, Ou J, et al. Genetic landscape and autoimmunity of monocytes in developing Vogt-Koyanagi-Harada disease. Proc Natl Acad Sci U S A. 2020;117(41):25712–21.
58. Szabo PA, Levitin HM, Miron M, Snyder ME, Senda T, Yuan J, Cheng YL, Bush EC, Dogra P, Thapa P, et al. Single-cell transcriptomics of human T cells reveals tissue and activation signatures in health and disease. Nat Commun. 2019;10(1):4706.
59. Kaser T, Mair KH, Hammer SE, Gerner W, Saalmuller A. Natural and inducible Tregs in swine: Helios expression and functional properties. Dev Comp Immunol. 2015;49(2):323–31.
60. Brandt D, Hedrich CM. TCRalphabeta(+)CD3(+)CD4(-)CD8(-) (double negative) T cells in autoimmunity. Autoimmun Rev. 2018;17(4):422–30.
61. Zuckermann FA, Husmann RJ. Functional and phenotypic analysis of porcine peripheral blood CD4/CD8 double-positive T cells. Immunology. 1996;87(3):500–12.
62. Sedlak C, Patzl M, Saalmuller A, Gerner W. CD2 and CD8alpha define porcine gammadelta T cells with distinct cytokine production profiles. Dev Comp Immunol. 2014;45(1):97–106.
63. Stepanova K, Sinkora M. Porcine gammadelta T lymphocytes can be categorized into two functionally and developmentally distinct subsets according to expression of CD2 and level of TCR. J Immunol. 2013;190(5):2111–20.
64. Sedlak C, Patzl M, Saalmuller A, Gerner W. IL-12 and IL-18 induce interferon-gamma production and de novo CD2 expression in porcine gammadelta T cells. Dev Comp Immunol. 2014;47(1):115–22.
65. Rodriguez-Gomez IM, Talker SC, Kaser T, Stadler M, Hammer SE, Saalmuller A, Gerner W. Expression of T-bet, Eomesodermin and GATA-3 in porcine alpha-beta T cells. Dev Comp Immunol. 2016;60:115–26.
66. Rodriguez-Gomez IM, Talker SC, Kaser T, Stadler M, Reiter L, Ladinig A, Milburn JV, Hammer SE, Mair KH, Saalmuller A, et al. Expression of T-Bet, Eomesodermin, and GATA-3 Correlates With Distinct Phenotypes and Functional Properties in Porcine gammadelta T Cells. Front Immunol. 2019;10:396.
67. Melichar HJ, Narayan K, Der SD, Hiraoka Y, Gardiol N, Jeannet G, Held W, Chambers CA, Kang J. Regulation of gammadelta versus alphabeta T lymphocyte differentiation by the transcription factor SOX13. Science. 2007;315(5809):230–3.
68. Lanier LL. NKG2D Receptor and Its Ligands in Host Defense. Cancer Immunol Res. 2015;3(6):575–82.
69. Xu AQ, Barbosa RR, Calado DP. Genetic timestamping of plasma cells in vivo reveals tissue-specific homeostatic population turnover. Elife. 2020;9:e59850.
70. Liu B, Li Z. Endoplasmic reticulum HSP90b1 (gp96, grp94) optimizes B-cell function via chaperoning integrin and TLR but not immunoglobulin. Blood. 2008;112(4):1223–30.
71. Andreani V, Ramamoorthy S, Pandey A, Lupar E, Nutt SL, Lammermann T, Grosschedl R. Cochaperone Mzb1 is a key effector of Blimp1 in plasma cell differentiation and beta1-integrin function. Proc Natl Acad Sci U S A. 2018;115(41):E9630–9.
72. Rahe MC, Dvorak CMT, Wiseman B, Martin D, Murtaugh MP. Establishment and characterization of a porcine B cell lymphoma cell line. Exp Cell Res. 2020;390(2):111986.
73. Schneider WM, Chevillotte MD, Rice CM. Interferon-stimulated genes: a complex web of host defenses. Annu Rev Immunol. 2014;32:513–45.
74. Gyory I, Boller S, Nechanitzky R, Mandel E, Pott S, Liu E, Grosschedl R. Transcription factor Ebf1 regulates differentiation stage-specific signaling, proliferation, and survival of B cells. Genes Dev. 2012;26(7):668–82.
75. Fedl AS, Tagoh H, Gruenbacher S, Sun Q, Schenk RL, Froussios K, Jaritz M, Busslinger M, Schwickert TA. Transcriptional function of E2A, Ebf1, Pax5,

Ikaros and Aiolos analyzed by in vivo acute protein degradation in early B cell development. Nat Immunol. 2024;25(9):1663–77.
76. Kurotaki D, Sasaki H, Tamura T. Transcriptional control of monocyte and macrophage development. Int Immunol. 2017;29(3):97–107.
77. Odumade OA, Weinreich MA, Jameson SC, Hogquist KA. Kruppel-like factor 2 regulates trafficking and homeostasis of gammadelta T cells. J Immunol. 2010;184(11):6060–6.
78. Carlson CM, Endrizzi BT, Wu J, Ding X, Weinreich MA, Walsh ER, Wani MA, Lingrel JB, Hogquist KA, Jameson SC. Kruppel-like factor 2 regulates thymocyte and T-cell migration. Nature. 2006;442(7100):299–302.
79. Li W, Zhang Z, Kumar S, Botey-Bataller J, Zoodsma M, Ehsani A, Zhan Q, Alaswad A, Zhou L, Grondman I, et al. Single-cell immune aging clocks reveal inter-individual heterogeneity during infection and vaccination. Nat Aging. 2025;5(4):607–21.
80. Pizzolato G, Kaminski H, Tosolini M, Franchini D-M, Pont F, Martins F, Valle C, Labourdette D, Cadot S, Quillet-Mary A, et al. Single-cell RNA sequencing unveils the shared and the distinct cytotoxic hallmarks of human TCRVδ1 and TCRVδ2 γδ T lymphocytes. Proc Natl Acad Sci U S A. 2019;116(24):11906–15.
81. Tian D, Pan Y, Zhao Y, Wang H, Tian Y, Yang L, Shi W, Zhang C, Zhu Y, Zhang Y, et al. TCRαβ + NK1.1-CD4-CD8- double-negative T cells inhibit central and peripheral inflammation and ameliorate ischemic stroke in mice. Theranostics. 2023;13(3):896–909.
82. Zuckermann FA. Extrathymic CD4 CD8 double positive T cells. Vet Immunol Immunopathol. 1999;72(1–2):55–66.
83. Laux I, Khoshnan A, Tindell C, Bae D, Zhu X, June CH, Effros RB, Nel A. Response differences between human CD4(+) and CD8(+) T-cells during CD28 costimulation: implications for immune cell-based therapies and studies related to the expansion of double-positive T-cells during aging. Clin Immunol. 2000;96(3):187–97.
84. Lee WW, Nam KH, Terao K, Akari H, Yoshikawa Y. Age-related increase of peripheral CD4 + CD8+ double-positive T lymphocytes in cynomolgus monkeys: longitudinal study in relation to thymic involution. Immunology. 2010;109(2):217–25.

## Publisher's note